이학박사학위논문

알츠하이머병의 타우 단백질 병증에서 ALK에 대한 연구

Studies on the role of ALK in tau proteinopathy and its implications in Alzheimer's disease

2020년 2월

서울대학교 대학원

생명과학부

박 지 수

알츠하이머병의 타우 단백질 병증에서 ALK에 대한 연구

Studies on the role of ALK in tau proteinopathy and its implications in Alzheimer's disease

지도교수 정 용 근

이 논문을 이학박사 학위논문으로 제출함

2019년 12월

서울대학교 대학원
생명과학부

박 지 수

박지수의 이학박사 학위논문을 인준함
2019년 12월

위 원 장 최 석 우 (인)

부위원장 정 용 근 (인)

위 원 노 성 훈 (인)

위 원 조 동 규 (인)

위 원 김 대 영 (인)

Studies on the role of ALK in tau proteinopathy and its implications in Alzheimer's disease

A dissertation submitted in partial fulfillment of the requirement for the degree of

DOCTOR OF PHILOSOPHY

To the Faculty of

School of Biological Sciences

at

SEOUL NATIONAL UNIVERSITY

by

Jisu Park

Date Approved:
December, 2019

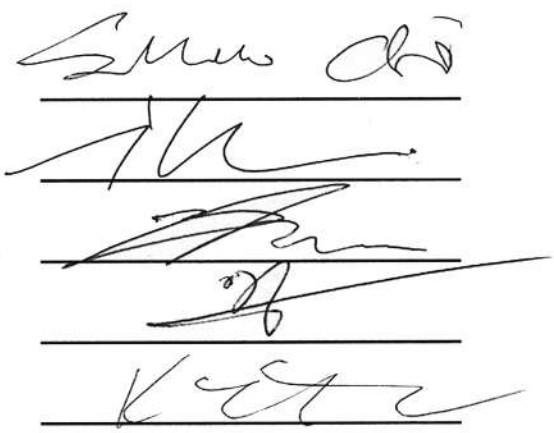

ABSTRACT

Studies on the role of ALK in tau proteinopathy and its implications in Alzheimer's disease

Jisu Park

School of Biological Sciences

The Graduate School

Seoul National University

Neurodegenerative diseases are characterized by formation of specific protein aggregates. Alzheimer's disease, the most prevalent tauopathy and common cause of dementia, exhibit abnormal accumulation of tau protein and deposition of tau tangles. Tau, a microtubule-binding protein, is phosphorylated by various kinases such as GSK3β, ERK and CDK5. Highly phosphorylated tau dissociates with microtubules and accumulates to form neurofibrillary tangles. Modified tau protein exerts it toxicity via microtubule disassembly, altered signaling, synaptic and mitochondrial dysfunction.

Despite active identification of tau modifications and mutations responsible for tau aggregation, a critical modulator inducing tau pathology by affecting its protein modification-degradation flux is not known. Here, I demonstrate that anaplastic lymphoma kinase (ALK), a receptor tyrosine kinase, is responsible for the tau-mediated AD pathology and identify prospecting ALK inhibitors and putative ALK agonistic antibodies.

ALK is a receptor tyrosine kinase (RTK) that belongs to the insulin receptor superfamily. Aberrant ALK activity has been highly implicated in the oncogenesis of human cancer as a fusion protein in inflammatory myofirbroblastic tumor, diffuse large B-cell lymphoma and anaplastic large-cell lymphoma (ALCL) or through mutations in full-length protein in hereditary familial neuroblastoma. Thus, ALK is being employed as a therapeutic target for the prevention of cancer. On the other hand, its role in the neurodegeneration and AD pathology is not known.

In chapter 1, I report that ALK is responsible for the tau-mediated AD pathology. Through cell-based functional screening using human 650 kinase cDNAs in hippocampal HT22 cells, ALK, a neuronal receptor tyrosine kinase, was selected to increase the level of phosphorylated form of tau. ALK caused abnormal hyperphosphorylation of tau and its accumulation in the somatodendritic region of neurons through its tyrosine kinase activity, while

tau levels were reduced in the brains of *Alk* knockout mice. Notably, ALK activation in neurons impaired autophagosome maturation and this defect was reversed by dominant-negative Grb2. ALK induced LC3-positive axon swelling and loss of spine density, leading to tau-dependent neuronal degeneration. ALK levels were significantly elevated in the brains of AD patients, and injection of an ALK.Fc-lentivirus exacerbated memory impairment in 3xTg-AD mice. Conversely, administration of ALK inhibitors reversed the memory impairment and tau accumulation in both 3xTg-AD and tauC3 mice. Together, I propose that aberrantly activated ALK is a bona fide mediator of a proteinopathy that disrupts autophagosome maturation and causes tau accumulation, leading to neuronal dysfunction in AD.

Further research attempted to find tools regulating ALK activity. In chapter 2, I identified prospecting non-active site ALK inhibitors and putative ALK agonistic antibodies, and also demonstrated *in vivo* effect of KRCA0605, ALK inhibitor targeting its kinase activity. Using Gal4-UAS system, 5 putative ALK inhibitors were identified in the screening. Those compounds inhibit ALK acitivty and ALK-mediated tau accumulationand aggregation in cell based-assay. Those inhibitors is proved to regulate ALK activity by targeting non-active site via *in vitro* kinase assay. In addiftion, I investigated the *in vivo* effect of another ALK inhibitor, KRCA0605 which is initially

developed for treating cancers, on memory defects and tau accumulation of 3xTg-AD mice. As expected, oral administration of KRCA0605 diminished memory impairment and tau accumulation in the AD mice model. Lastly, I demonstrated the interaction between human ALK and putative ALK antibodies which are identified via phage antibody spanning. I also found that at least two of them function as agonistic antibodies, thus activate ALK activity and increases tau protein in cells. Taken together, I discovered inhibitors and antibodies to manipulate ALK activity, thus provide useful tools for manipualting ALK functions.

Key Words: ALK, Tau proteinopathy, Autophagosomal dysfunction, Alzheimer's Disease

Student Number: 2012-23066

CONTENTS

LIST OF FIGURES

ABBREVIATION

AD	Alzheimer's disease
ALK	Anaplastic lymphoma kinase
Aβ	Amyloid beta
Tg	Transgenic
GFP	Green-fluorescence protein
RFP	Red-fluorescence protein
TM	Transmembrane
WT	Wild-type
KO	Knockout
TREM2	Triggering receptor expressed on myeloid cells 2
IP	Immunoprecipitation
G418	Geneticin
HA	Hemagglutinin
LC3	Microtubule associated protein 1 light chain 3
GRB2	Growth factor receptor bound protein 2

UVRAG	UV radiation resistance associated
ULK1	Unc-51 like autophagy activating kinase 1
ECM	Extracellular membrane
DIV	Day *in vitro*
AL	Autolysosome
AP	Autophagosome
BSA	Bovine serum albumin
PBS	Phosphate buffered saline
EDTA	Ethylenediaminetetraacetic acid
DMSO	Dimethyl sulfoxide
SDS	Sodium dodecyl sulfate
PAGE	Polyacrylamide gel electrophoresis
FITC	Fluorescein isothiocyanate
GSK3β	Glycogen synthase kinase 3 beta
CDK5	Cyclin dependent kinase 5
ERK	Extracellular signal-regulated kinase 2

MAPK	Mitogen-activated protein kinase
FACS	Fluorescence-activated cell sorting

CHAPTER I

Pathogenic role of ALK in tau-mediated neurodegeneration through autophagosomal dysregulation

Abstract

The formation of tangle is one of the main pathologic hallmarks of tauopathy, including Alzheimer's disease (AD). Tau, a microtubule assembly factor, functions in the stabilization of microtubules and the regulation of motor-driven axonal transport. Tau phosphorylation by kinases including GSK3β, CDK5, ERK and MAPK leads to its accumulation in the somatodendritic compartment of neurons, forming aggregates and neurofibrillary tangles (NFTs) at last. Those aggregates and NFTs are neurotoxic and result in neuronal cell death.

Although many efforts have been put on the identification of many kinases and phosphatases responsible for tau modifications, little is known about membrane receptor modulating tau pathology.

Here I report that ALK is a novel receptor responsible for tau pathology. ALK activation causes tau accumulation in neuronal cell lines and primary neurons. *Alk* KO mice have a lower level of total tau in cortical and hippocampal tissues than littermate WT mice. The tauopathic effect of ALK relies on its tyrosine kinase activity. Interestingly, we found that autophagosome maturation was impaired in neurons expressing ALK, leading to accumulation and re-localization of tau to the somatodendritic region of the neurons. ALK is able to interact with Grb2 and the ability of ALK to

inhibit maturation of autophagosome is dependent on Grb2, a SH2 domain protein. In addition, ALK causes LC3-positive exon swelling and decreases dendritic spine density, leading to neuronal cell death. AD patients have a 5-fold higher level of ALK in hippocampal tissues compared to elderly control. Injection of ALK.Fc lentivirus accelerates memory loss and tau phosphorylation in 3xTg-AD mice. Meanwhile, the respective administration of two different ALK inhibitors, NVP-TAE 684 and LDK378, into two different AD model mice, TauC3 and 3xTg-AD, recovers the memory impairment and decreases tau phosphorylation. Together, we propose that ALK is a bona fide plasma membrane protein responsible for tau pathology.

Introduction

Accumulation of protein aggregates is a shared feature of neurodegenerative disorders. Among these are the tauopathies, which exhibit accumulation of tau protein (Lee, Goedert, and Trojanowski 2001) and include Alzheimer's disease (AD), progressive supranuclear palsy, Pick's disease, corticobasal degeneration and frontotemporal dementia with parkinsonism linked to chromosome 17 (FTDP-17) (Bergeron et al. 1997; Bugiani et al. 1999; Delacourte et al. 1998; Ittner and Gotz 2011). AD, the most common cause of dementia, is characterized by the deposition of intracellular tau tangles. Abnormally phosphorylated tau is cleared via an autophagic process involving autophagosome-dependent, lysosome-mediated degradation. Otherwise, the protein mislocalizes and accumulates within neurons (Kruger et al. 2012). Although it has been proposed that tau functions exclusively downstream of amyloid-beta (Aβ) (Ittner et al. 2010; Roberson et al. 2007), an increasing number of studies have found that tau is able to exert adverse effects on neurons independently of or dominantly over Aβ (Busche et al. 2019). Moreover, ApoE and TREM2, the most well-known risk factors for sporadic AD, are highly associated with tau-mediated pathology, deteriorating tau-induced neurotoxicity in a mouse model of tauopathy (Shi et al. 2017), and worsening gliosis and inflammation related to tau-mediated

neuronal damage (Bemiller et al. 2017; Leyns et al. 2017). Despite many studies focusing on tau modification and aggregation, a crucial receptor that regulates tau accumulation, clearance and pathology beyond that mentioned above remains elusive.

Anaplastic lymphoma kinase (ALK) is a receptor tyrosine kinase belonging to the insulin receptor superfamily (Iwahara et al. 1997; Morris et al. 1997). ALK has a restricted distribution in mammals, being found at significant levels mainly in the central nervous system during development (Iwahara et al. 1997; Vernersson et al. 2006). Aberrant ALK activity has been strongly implicated in the oncogenesis of human cancer as a fusion protein in inflammatory myofibroblastic tumors, diffuse large B-cell lymphoma and anaplastic large-cell lymphoma, or through mutations in the full-length protein in hereditary familial neuroblastoma (Chen et al. 2008; George et al. 2008; Morris et al. 1994; Childress et al. 2015; Hapgood and Savage 2015). This makes ALK a therapeutic target in cancer (Galkin et al. 2007; Zou et al. 2007; Shaw et al. 2014a). More recent evidence also indicates that ALK may regulate the STING pathway and innate immune responses (Zeng et al. 2017). A low level of ALK expression is maintained in the adult brain and *Alk* knockout mice display a full life span (Bilsland et al. 2008). However, its role in neurodegeneration and AD pathology is not known.

Here, I report that ALK mediates tau pathology. ALK activation induced

tau phosphorylation and impaired autophagosome maturation, thereby preventing degradation and accelerating the aggregation of abnormally phosphorylated tau. In *Drosophila melanogaster* ALK exacerbated the tau rough eye phenotype. In the 3xTg-AD and TauC3 mouse AD models, ALK exacerbated tau-related memory deficits, while its pharmacological inhibition restored memory in the model mice. Our results define a crucial role of ALK in tau-mediated neurodegeneration and provide insight into the pathogenesis of AD and a new approach to AD therapeutics.

Results

Neuronal ALK promotes the accumulation and aggregation of phosphorylated tau

To identify novel regulators functioning in tau-mediated pathogenesis, we established a cell-based tau aggregation assay. Ectopic expression of GFP-tagged and caspase-cleaved tau (GFP-tauD421) resulted in the formation of green fluorescence- and thioflavin S-positive tau aggregates in HT22 mouse hippocampal neuronal cells. Utilizing this assay, we functionally screened approximately 2,600 cDNAs encoding 630 kinases and 2,000 membrane proteins, and isolated a list of putative positive clones that affected tau aggregation following ectopic expression of these cDNAs. Among them, mouse ALK most effectively increased tau aggregation in the transfected cells.

Like mouse ALK, infection of primary hippocampal neurons with a lentivirus carrying constitutively active ALK.Fc, a chimeric protein in which the extracellular domain of human ALK was replaced by the mouse IgG 2b Fc domain for dimerization (Moog-Lutz et al. 2005) (Figure I-1A), dramatically increased accumulation of phosphorylated tau (Figure I-1B, C). By contrast, the kinase-dead ALK.Fc KD mutant exhibited no such stimulatory activity. Likewise, treating primary hippocampal neurons with mAb46, an agonistic ALK antibody (Moog-Lutz et al. 2005), increased tau

levels and its phosphorylation, while pre-treatment with mAb30, an antagonistic ALK antibody (Moog-Lutz et al. 2005), blocked mAb46-mediated tau accumulation (Figure I-1D). That overexpressed ALK did not affect tau mRNA levels (data not shown) suggests the increase in tau protein levels (approximately ~5-fold) by ALK reflects a posttranslational event. This was confirmed by our observation that ALK.Fc enhanced the stability of tau protein in HT22 cells (Figure I-2).

In AD, tau accumulation is accompanied by abnormal phosphorylation at many epitopes (Li and Gotz 2017). We found that ALK phosphorylated human and mouse tau at multiple serine and threonine residues, including the AD epitopes PHF-1 (S396/S404), 12E8 (S262/S356), CP13 (S202) and pThr231-tau (Figure I-1 B-D). In addition, ALK altered the subcellular localization of tau in primary neurons. The phosphorylated tau was apparently relocalized from the axon to the somatodendritic region following expression of ALK.Fc (Figure I-3). ALK knockdown decreases tau levels in SH-SY5Y cells (Figure I-4). In addition, exploration of tau levels in the brain tissues from *Alk* knockout mice and their wild-type littermates at different ages revealed that genetic ablation of *Alk* reduced tau protein levels in the mouse cortex and hippocampus (Figure I-5). Collectively, these findings indicated that ALK stimulates tau stabilization and hyperphosphorylation in neuronal cells through its kinase activity.

ALK impairs autophagosome maturation to accumulate tau protein via Grb2

The finding that ALK enhances levels of both tau protein and its aggregation led us to ask whether ALK plays a role in the degradation and/or clearance of tau. ALK.Fc expression did not directly affect proteasome activity (Figure I-6). Interestingly, ALK.Fc led to increased levels of p62, an autophagosome substrate, and LC3-I/II, two autophagosome markers (Yoshii and Mizushima 2017), as well as tau (Figure I-7). ALK.Fc did not phosphorylate activatory site at Ser555 of ULK1, an initiator Ser/Thr kinase of autophagy (Egan et al. 2011), or the level of Beclin1, a component of VPS34 complexes (Kang et al. 2011). Overexpression of ALK has no effect on lysosomal activity (Figure I-8). Thus, it is likely that ALK impairs autophagic flux by blocking a late step in the autophagic process. As expected, mCherry-GFP LC3 assays revealed that ALK increased numbers of GFP-positive autophagosomes but decreased numbers of autolysosome (Figure I-9). In addition, ALK.Fc, but not inactive ALK, interfered with the colocalization of GFP-Stx17, a SNARE that guides autophagosomes to lysosomes for fusion (Itakura, Kishi-Itakura, and Mizushima 2012), with RFP-LC3-positive dots (Figure I-10). Thus, ALK activation leads to impairment in autophagosome maturation. UVRAG is a membrane trafficking protein and its complex is involved in several steps of

autophagy. UVRAG makes a core complex with Belin1, Vps34, and p150, and temporarily interacts with p-Bif and Rubicon. The core complex enhances autophagosome maturation and endosome maturation. While the p-Bif-bound complex promotes autophagosome formation, binding with Rubicon interferes with autophagosome maturation and endosome maturation. I investigated the effect of ALK on UVRAG complex, however, ALK.Fc did not affect the interaction of Beclin1 with UVRAG (Figure I-11).

Up to now, no downstream mediator of ALK has provided a clue to the mechanism underlying ALK-induced autophagosomal defects. Upon activation, ALK is autophosphorylated at key tyrosine residues in its cytosolic domain to create specific sites for the assembly of downstream signaling adaptors harboring Src homology 2 (SH2) and phosphotyrosine binding (PTB) domains (Wagner et al. 2013). Therefore, I screened 108 dominant-negative (DN) forms of the proteins to isolate the SH2 domain-containing adaptors that affect tau accumulation.

From this screening, I identified DN forms of Grb10, PLCG1, Grb2, and Fyn (Figure I-12). Among them, Fyn is reported to upregulate the transcriptional level of tau and enhance the somatodendritic accumulation of tau via ERK-S6 signaling. Also, Fyn is relocated toward dendritic spins by interacting with tau and mediates Aβ-induced neuronal toxicity. Thus, I investigated the involvement of Fyn in ALK-mediated tau accumulation. Fyn

knockdown in SH-SY5Y cells inhibited ALK-induced tau aggregation and accumulation (Figure I-13A-C). Treatment of PP2, a Src-family inhibitor, hindered tau phosphorylation and accumulation in a dose-dependent manner (Figure I-14A). As in the previous screening, two Fyn DN forms suppressed ALK-mediated tau phosphorylation, tau accumulation and cell death (Figure I-14B, C). Furthermore, overexpressed Fyn interacts with overexpressed ALK (Figure I-15A, B). However, I failed to observe that ALK activation phosphorylates and activates Fyn (Figure I-15C). Therefore, I decided to focus on other DN forms of SH2 proteins discovered by the screening. Overexpression of those three dominant negatives (GRB10, PLCG1, GRB2) seemed to reverse ALK-mediated accumulation of tau and p62, and LC3 conversion (Figure I-16A). Among them, Grb2-DN also restored the colocalization of BFP-Stx17 and RFP-LC3 in SH-SY5Y/ALK stable cells (Figure I-16 B). I also found that Grb2 was able to interact with ALK (Figure I-16C). These results demonstrate that ALK interferes with autophagosome maturation in a Grb2-dependent manner, causing tau protein to accumulate in neurons.

ALK induces deterioration of axons and dendritic spines, making neurons vulnerable to death

When immature autophagosomes fail to fuse with lysosomes, both the

autophagosomes and lysosomes pile up (Chen et al. 2012). The excess autophagosomes/lysosomes cause axonal swelling, followed by retraction and neuronal death (Ivankovic et al. 2019). ALK.Fc caused LC3-positive neurons to undergo massive axonal swelling (Figure I-17A). In addition, the spine density on primary hippocampal neurons was significantly reduced by treatment with the agonistic ALK antibody mAb46, but not the antagonistic ALK antibody mAb30, and the mAb46-induced reduction in spine density was effectively blocked by the ALK inhibitors NVP-TAE684 and PF-2341066 developed by Novartis and Pfizer (Galkin et al. 2007; Zou et al. 2007), respectively (Figure I-17B).

Because neuronal cells undergoing neurodegeneration are susceptible to cell death, I directly assessed the effects of ALK on neuronal cell death. Treatment with the agonistic ALK antibody mAb46 also induced a significant amount of cell death among primary hippocampal neurons (Figure I-18A). In addition, a dominant-negative form of Grb2 attenuated ALK-mediated cell death (Figure I-18B). I therefore concluded that by inducing axonal deterioration and reductions in spine density, ALK reduces neuronal viability in a tau-dependent manner.

Increased ALK exacerbates memory impairment in 3xTg-AD mice

As reported, ALK expression was ubiquitously found in the adult mouse brain,

including cortex and hippocampus, and in the purified hippocampal neurons. When I also analyzed ALK expression in the brains of patients with AD, I found that ALK was elevated by 5-fold in hippocampal tissues in patients with AD as compared to elderly controls and that this elevation of ALK was highly correlated with tau phosphorylation and p62 accumulation (Figure I-19A). In addition, immunohistochemistry of the cortical region of patients with AD revealed that ALK immunoreactivity colocalized with the neurofibrillary tangles detected by antibodies against the phosphorylated tau (Figure I-19B). ALK is thus aberrantly increased in the AD brains showing tau and p62 accumulation.

I next addressed the effect of increased ALK on AD pathology using 3xTg-AD model mice, which express APP, PS and tau in neuronal cells (Sterniczuk et al. 2010). I designed a lentivirus encoding both GFP and ALK.Fc (Motegi et al. 2004) and stereotaxically injected the ALK.Fc-lentivirus into the dentate gyrus of 5- to 6-month-old 3xTg-AD mice. Behavioral tests performed by the mice one month after the injection revealed that spatial memory was greatly impaired by the delivery of the ALK.Fc-lentivirus (Figure I-20A). Similarly, a noble object recognition test and a passive avoidance test respectively revealed exacerbated reductions in object recognition memory and the discrimination index in 3xTg-AD mice (Figure I-20B, C). Unexpectedly, I observed noticeable memory impairment in age-

matched wild-type (WT) mice after injection with ALK.Fc-lentivirus. Using western blot analysis, I confirmed expression of the Venus and tau (Tau 12) transgenes in the injected tissue and found increased phosphorylation (PHF1 and CP13) of tau after ALK.Fc expression in the hippocampal tissues of both WT and 3xTg-AD mice (Figure I-20D). These results suggest that the increased ALK levels worsen memory function in 3xTg-AD mice and increases abnormal tau phosphorylation.

Pharmacological inhibition of ALK reverses tau pathologies in two AD model mice

I also tested whether ALK inhibition would affect memory function in two models of AD: TauC3 and 3xTg-AD mice. TauC3 is a caspase-cleaved form of tau (1-420) detected in the brains of patients with AD (Chung et al. 2001; Kim, Choi, et al. 2016). Transgenic mice expressing TauC3 under the brain-specific angiogenesis inhibitor 1-associated protein 4 (BAI1-AP4) promoter exhibit rapidly developing memory impairment at a young age with a concomitant increase in tau oligomers (Kim, Choi, et al. 2016). Because PF-2341066 does not cross the brain-blood barrier (B.B.B.), I directly delivered the ALK inhibitor into the brains of TauC3 mice through intracerebroventricular injection (Kam et al. 2013). After 3 weeks of injections, the results of behavioral tests revealed that PF-2341066 blocked

the impairment of spatial memory, object recognition memory and the discrimination index otherwise seen in TauC3 mice (Figure I-21A-C). In addition, western blotting showed that the tau phosphorylation (PHF1, T231, CP13, 12E8) observed in control TauC3 mice was inhibited by the treatment with PF-2341066 (Figure I-21D). Thus, ALK plays a role in the impaired memory function and abnormal tau phosphorylation in TauC3 model mice.

LDK378 (Ceritinib) is a recently developed ALK inhibitor that is highly permeable to the B.B.B. and used in the treatment of brain cancer (Kim, Mehra, et al. 2016). Prior to *in vivo* test of LDK378, the inhibiting effect of LDK378 was verified in neuronal cell line SH-SY5Y. LDK378 prevented phosphorylation of ALK and ERK, its downstream effecter, and ALK-induced p62 accumulation (Figure I-22). I tested the effect of LDK378 on the memory function in 6-month-old 3xTg-AD model mice. The mice were intraperitoneally injected with LDK378 daily for four weeks and then analyzed. Consistent with the results observed in TauC3 mice, LDK378 dramatically rescued the memory functions in 3xTg-AD mice, as assayed using the Y-maze, noble object recognition and passive avoidance tests (Figure I-23A-C). At the same time, LDK378 administration inhibited tau phosphorylation at multiple epitopes (PHF-1, CP13) as well as tau accumulation (HT7) in the brains of the mice (Figure I-23D, E). All these results point to the critical role played by ALK in the phosphorylation and

accumulation of tau and in the associated memory impairment seen in 3xTg-AD mice.

Figure I-1. ALK increases tau level in primary neurons.

(A) Schematic diagram of the wild-type and mutant ALK constructs. Arrowheads indicate kinase-dead (KD) mutants, and IgG Fc is the Fc region of immunoglobulin G. (B-D) ALK-induced increases in tau accumulation, phosphorylation, and aggregation. Mouse primary hippocampal neurons (DIV13) were infected with control vector, ALK.Fc or ALK.Fc KD lentivirus (MOI5) and maintained for 8 days *in vitro* (B, C). Mouse primary hippocampal neurons (DIV7) were treated with 6 nM IgG, mAb30 (antagonistic antibody), mAb46 (agonistic antibody) or mAb46 following pre-incubation with mAb30 for 24 h (D). TG5, total tau; HT7, exogenous human tau; MC1, pathological tau; PHF-1, p-Tau Ser396/Ser404; CP13, p-Tau Ser202.

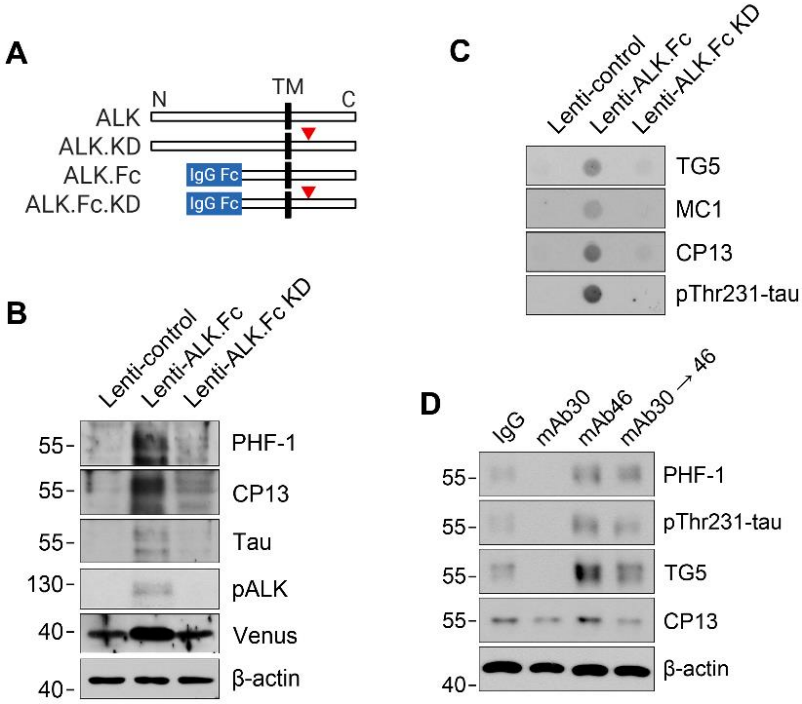
A
N
TM
C
ALK
ALK.KD
ALK.Fc
IgG Fc
ALK.Fc.KD
IgG Fc
B
Lenti-control
Lenti-ALK.Fc
Lenti-ALK.Fc KD
55-
PHF-1
55-
CP13
55-
Tau
130-
pALK
40-
Venus
40-
β-actin
C
Lenti-control
Lenti-ALK.Fc
Lenti-ALK.Fc KD
TG5
MC1
CP13
pThr231-tau
D
IgG
mAb30
mAb46
mAb30 → 46
55-
PHF-1
55-
pThr231-tau
55-
TG5
55-
CP13
40-
β-actin

Figure I-2. ALK enhances accumulation of tau proteins.

HT22 cells were transfected with GFP-tau and control vector (-) or ALK.Fc (+) construct. The relative ratios of the tau to β-actin signal were quantified by densitometric analysis ($n = 3$). Bars depict means ± S.D. $^{**}P < 0.01$; paired two-tailed *t*-test.

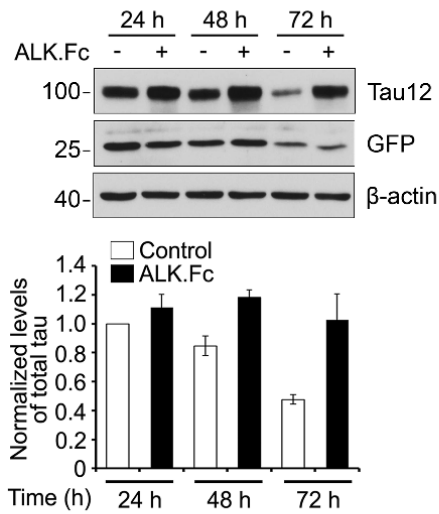
24 h
48 h
72 h
ALK.Fc
- + - + - +
100-
25-
40-
Tau12
GFP
β-actin
Control
ALK.Fc
Normalized levels of total tau
1.4
1.2
1.0
0.8
0.6
0.4
0.2
0
Time (h)
24 h
48 h
72 h

Figure I-3. ALK activation leads to tau relocalization in cultured neurons. Mouse primary hippocampal neurons (DIV 7) were transfected for 24 h with RFP-N1 plus control vector, ALK.Fc or ALK.Fc.KD and immunostained with anti-ALK (blue) or anti-tau (green) antibody, after which fluorescent signals were observed under a confocal microscope (upper). The relative immunoreactivity of total tau (A) and phosphorylated tau (B) were quantified by densitometric analysis (n = 10) (lower). Bars depict means ± S.E.M. $^{**}P < 0.01$, $^{***}P < 0.001$; one-way ANOVA followed by Tuckey's test.

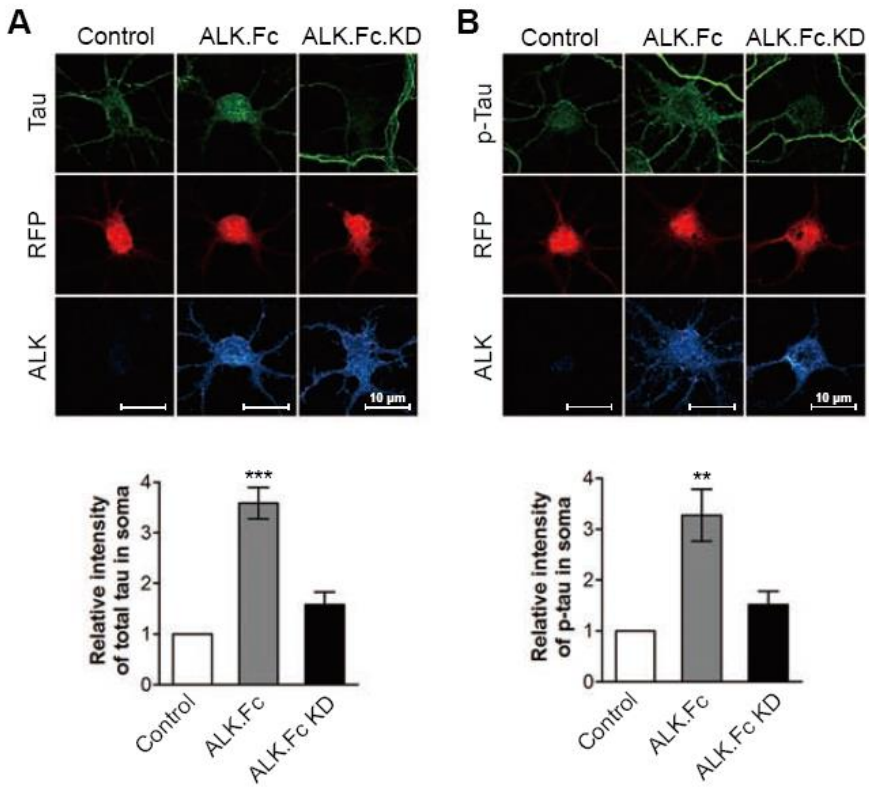
A
Control
ALK.Fc
ALK.Fc.KD
Tau
RFP
ALK
10 µm
B
Control
ALK.Fc
ALK.Fc.KD
p-Tau
RFP
ALK
10 µm
Relative intensity of total tau in soma
***
Control
ALK.Fc
ALK.Fc KD
Relative intensity of p-tau in soma
**
Control
ALK.Fc
ALK.Fc KD

Figure I-4. Knockdown of ALK decreases tau accumulation.

(A) SH-SY5Y cells were transfected for 48 h with Cas9/sgCon or Cas9/sgALK constructs, and then cells were cultured in selective medium. After 3 days of selection, cell lysates were subjected to Western blot analysis. (B) Mixed population of ALK knockdown SH-SY5Y cells were cotransfected for 24 h with GFP-tau and GFP-N1, and then subject to Western blot analysis.

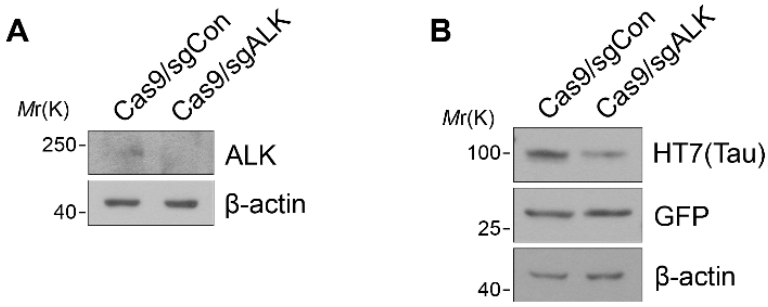
A
Cas9/sgCon
Cas9/sgALK
Mr(K)
250-
ALK
40-
β-actin
B
Cas9/sgCon
Cas9/sgALK
Mr(K)
100-
HT7(Tau)
25-
GFP
40-
β-actin

Figure I-5. Tau levels are decreased in brain tissues from *Alk* knockout mice.

Cortical and hippocampal tissues from wild-type (WT) and *Alk* knockout mice were analyzed by western blotting.

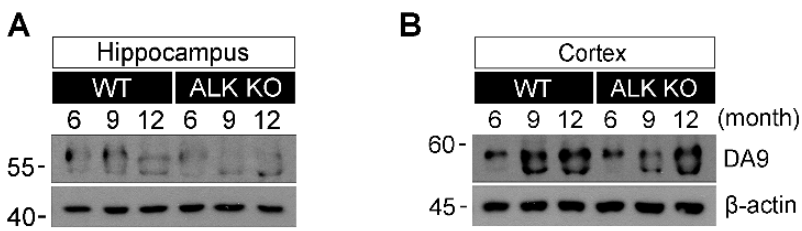
A
Hippocampus
WT
ALK KO
6 9 12 6 9 12
55-
40-
B
Cortex
WT
ALK KO
6 9 12 6 9 12 (month)
60-
45-
DA9
β-actin

Figure I-6. Overexpressed ALK does not affect the accumulation of the GFP^{u} degron.

HT22 cells were cotransfected for 24 h with GFP^{u} plus control vector, ALK.Fc or ALK.Fc KD, and then subjected to western blotting (A) or observed under a fluorescence microscope (B).

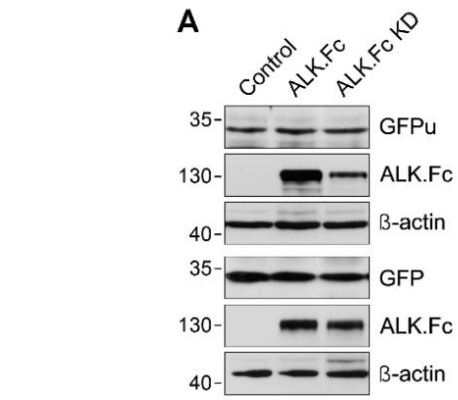
A
Control
ALK.Fc
ALK.Fc KD
35
GFPu
130
ALK.Fc
40
β-actin
35
GFP
130
ALK.Fc
40
β-actin

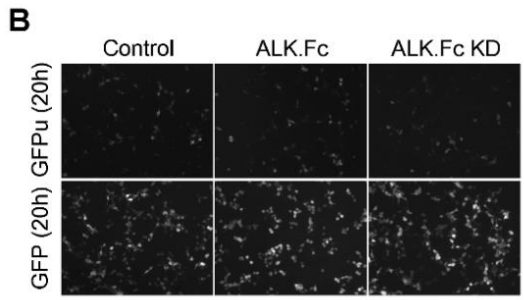
B
Control
ALK.Fc
ALK.Fc KD
GFPu (20h)
GFP (20h)

Figure I-7. ALK causes LC3 accumulation without affecting ULK1/Beclin1 activity.

SH-SY5Y cells expressing GFP-tau were transfected for 24 h with control vector, ALK.Fc or ALK.Fc.KD, and analyzed by western blotting (left). The signals on the blots were quantified by densitometric analysis ($n = 3$) (right). Bars depict means ± S.E.M. *$P < 0.05$ **$P < 0.01$, ***$P < 0.001$; one-way ANOVA followed by Tuckey's test.

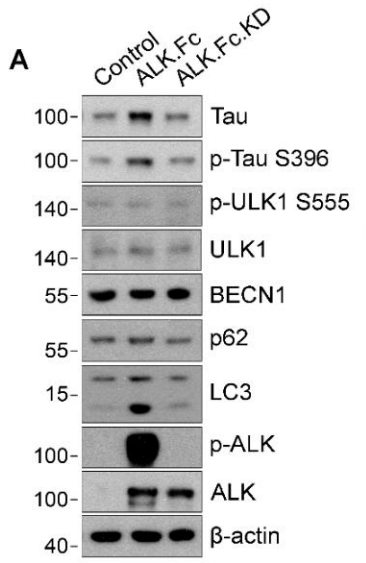
A
Control
ALK.Fc
ALK.Fc.KD
100
Tau
100
p-Tau S396
140
p-ULK1 S555
140
ULK1
55
BECN1
55
p62
15
LC3
100
p-ALK
100
ALK
40
β-actin

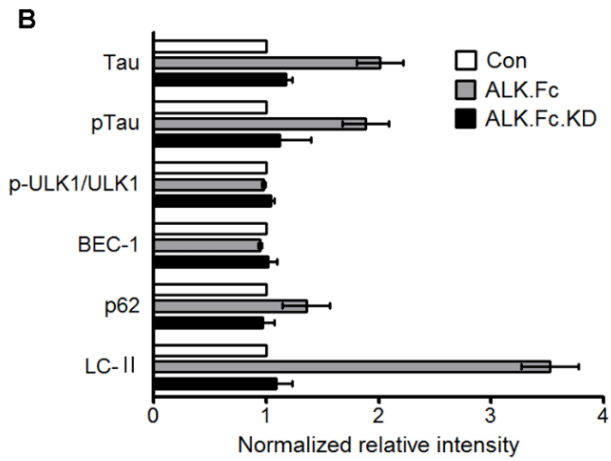
B
Tau
pTau
p-ULK1/ULK1
BEC-1
p62
LC-II
Con
ALK.Fc
ALK.Fc.KD
0
1
2
3
4
Normalized relative intensity

Figure I-8. Overexpression of ALK has no effect on lysosomal activity.

(A) Primary hippocampal neurons were cotransfected for 24 h with LAMP1-GFP plus control vector (Con), ALK.Fc or ALK.Fc.KD, and then stained with DQ-Red BSA for 6 h. The intensity of BODIPY TR-X fluorescence colocalized with LAMP1-GFP puncta was measured using a photoshop program. Data are presented as means ± S.E.M; one-way ANOVA followed by Tukey's test. (B) SH-SY5Y cells were cotransfected for 24 h with GFP-8, lysosome targeting sequence-harboring GFP (Perez-Sala et al. 2009), plus control vector (Con), ALK.Fc or ALK.Fc.KD, and then subjected to western blotting. CTSD, cathepsin D.

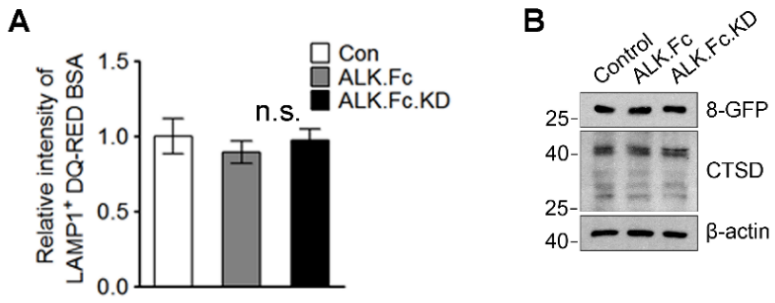
A
Relative intensity of LAMP1+ DQ-RED BSA
1.5
1.0
0.5
0.0
n.s.
Con
ALK.Fc
ALK.Fc.KD
B
Control
ALK.Fc
ALK.Fc.KD
25
40
25
40
8-GFP
CTSD
β-actin

Figure I-9. ALK impairs autophagic flux.

SH-SY5Y cells were transfected for 24 h with mCherry-LC3-GFP plus control vector, ALK.Fc or ALK.Fc.KD, and observed under a confocal microscope (left). The numbers of GFP (APs)- and mCherry (ALs)-positive dots per cell were quantified ($n > 30$ cells) (right). Bars depict means ± S.E.M. $^{**}P < 0.01$; one-way ANOVA followed by Tuckey's test.

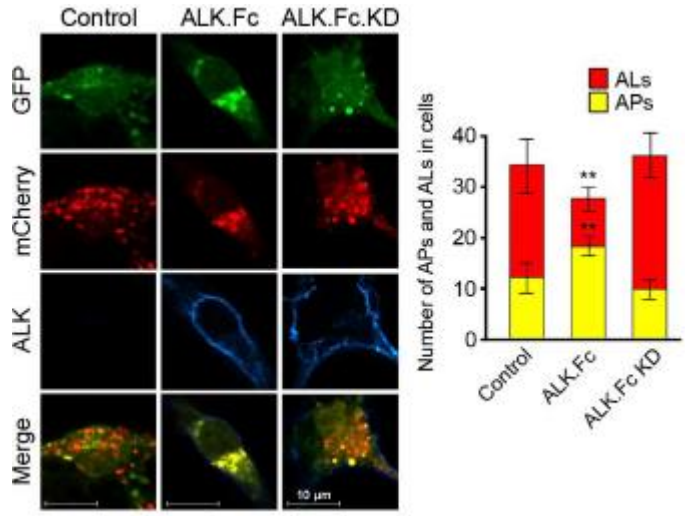
Control
ALK.Fc
ALK.Fc.KD
GFP
mCherry
ALK
Merge
10 μm
ALs
APs
Number of APs and ALs in cells
40
30
20
10
0
**
**
Control
ALK.Fc
ALK.Fc KD

Figure I-10. ALK decreases colocalization of GFP-Stx17 with RFP-LC3.

Mouse cortical neurons (DIV8) were transfected for 24 h with GFP-Stx17, RFP-LC3 and control vector, ALK.Fc or ALK.Fc.KD for (left). The percentages of GFP-positive RFP-LC3 dots among total LC3 dots (matured autophagosomes) were determined ($n > 30$) (right).

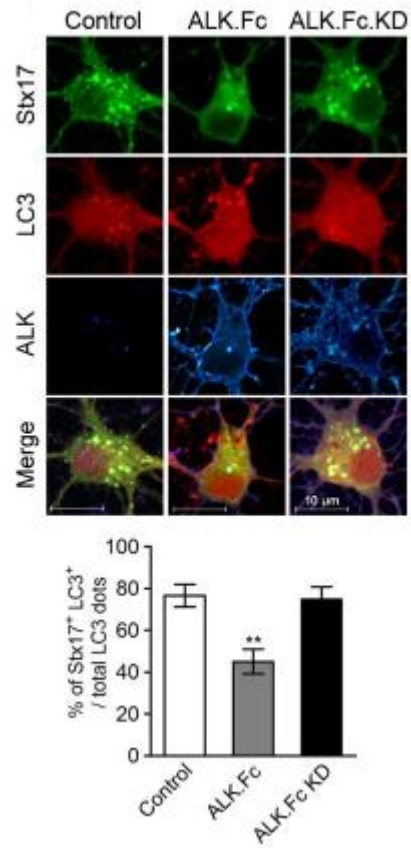
Control
ALK.Fc
ALK.Fc.KD
Stx17
LC3
ALK
Merge
10 µm
% of Stx17+ LC3+ / total LC3 dots
100
80
60
40
20
0
**
Control
ALK.Fc
ALK.Fc.KD

Figure I-11. ALK does not affect on Beclin 1/UVRAG complex.

SH-SY5Y cells were transfected for 24 h with control vector or ALK.Fc, and then lysates were immunoprecipitated (IP) with UVRAG antibody, and the immune complexes were assessed for the presence of Beclin 1 by Western blot (WB) with the antibody to Beclin 1.

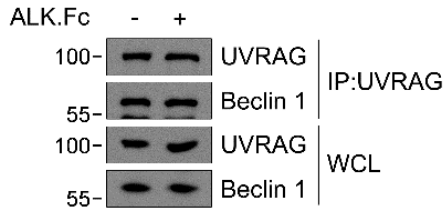
ALK.Fc
-
+
100-
UVRAG
55-
Beclin 1
IP:UVRAG
100-
UVRAG
55-
Beclin 1
WCL

Figure I-12. Isolation of a dominant-negative SH2 (SH2 DN) mutant interfering with ALK-induced tau accumulation.

SH-SY5Y cells were transfected with for 48 h ALK.Fc and each of 102 SH2 DN constructs for 24 h and then analyzed by western blotting.

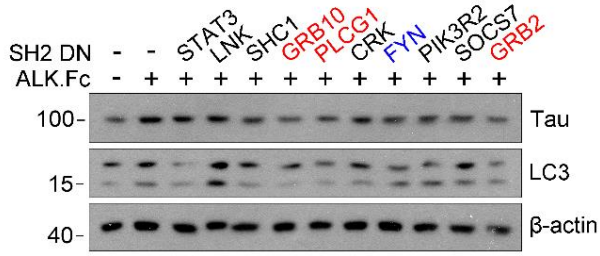
SH2 DN - - STAT3 LNK SHC1 GRB10 PLCG1 CRK FYN PIK3R2 SOCS7 GRB2
ALK.Fc - + + + + + + + + + + +
100-
Tau
15-
LC3
40-
β-actin

Figure I-13. Knockdown of Fyn attenuates ALK-mediated tau accumulation and aggregation.

(A) SH-SY5Y cells were transfected for 48 h with Cas9/sgCon or Cas9/sgFyn constructs, and then cells were cultured in selective medium. After 3 days of selection, cell lysates were subjected to Western blot analysis.

(B, C) SH-SY5Y cells stably expressing GFP-tau were transfected with either sgControl or indicated sgFyn constructs and with either pcDNA3.1 or ALK.Fc or ALK.Fc.KD. 48 h after the transfection, cells were subject to western blot analysis (B) and to filter trap assay (C).

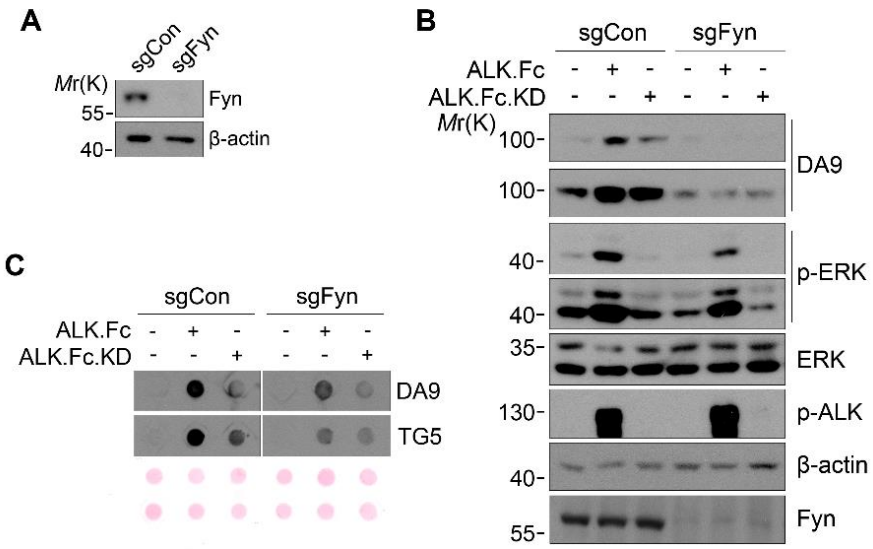
A
sgCon
sgFyn
Mr(K)
55-
40-
Fyn
β-actin
B
sgCon
sgFyn
ALK.Fc - + - - + -
ALK.Fc.KD - - + - - +
Mr(K)
100-
100-
DA9
40-
40-
p-ERK
35-
ERK
130-
p-ALK
40-
β-actin
55-
Fyn
C
sgCon
sgFyn
ALK.Fc - + - - + -
ALK.Fc.KD - - + - - +
DA9
TG5

Figure I-14. Inhibition of Fyn activity alleviates ALK-mediated tau accumulation and neuronal cell death.

(A) SH-SY5Y cells stably expressing GFP-tau were transfected with control vector or ALK.Fc and treated with indicated concentration of PP2. 48 h after the transfection, amounts of tau and phosphorylated tau in the cell extracts were determined with DA9 and CP13 antibodies, respectively.

(B) SH-SY5Y cells stably expressing GFP-tau were cotransfected with control vector or ALK.Fc and dominant negative forms of Fyn. 48 h after the transfection, cell lysates were subject to western blot analysis.

(C) HT22 cells were cotransfected with control vector or ALK.Fc and GFP-N1 or dominant negative form of Fyn. 48 h after the transfection, cell death was assessed by counting the number of GFP and EtHD18-positive cells after staining with 3 mg/ml ethidium homodimer at 37 °C for 15 min.

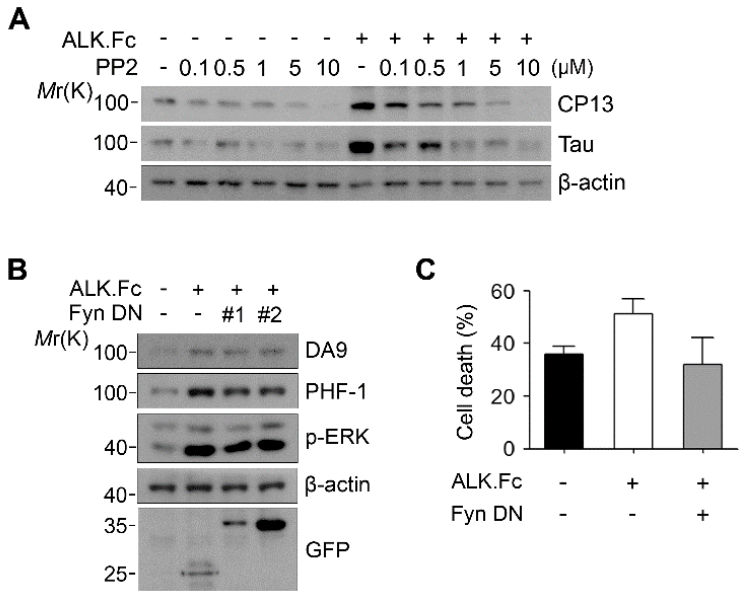
A
ALK.Fc - - - - - - + + + + + +
PP2 - 0.1 0.5 1 5 10 - 0.1 0.5 1 5 10 (μM)
Mr(K)
100-
CP13
100-
Tau
40-
β-actin
B
ALK.Fc - + + +
Fyn DN - - #1 #2
Mr(K)
100-
DA9
100-
PHF-1
40-
p-ERK
40-
β-actin
35-
25-
GFP
C
Cell death (%)
60
40
20
0
ALK.Fc - + +
Fyn DN - - +

Figure I-15. ALK interacts with Fyn, but is unable to phosphorylate and active Fyn.

(A, B) HEK293T cells were cotransfected with control vector or ALK or Fyn-FLAG. 24 h after the transfection, FLAG was immunoprecipitated (IP) with ALK antibody (A) or FLAG-M2 agarose beads (B), and the immune complexes were assessed for the presence of FLAG or ALK by Western blot with the antibody to FLAG (A) and ALK (B).

(C) HT22 cells were cotransfected with control vector, ALK.Fc, ALK.Fc.KD or Fyn-FLAG for 48 h. The transfected cells were lysed in RIPA buffer. Fyn was immunoprecipitated using anti-Fyn antibody. The immunoprecipitated complex was subject to western blot analysis.

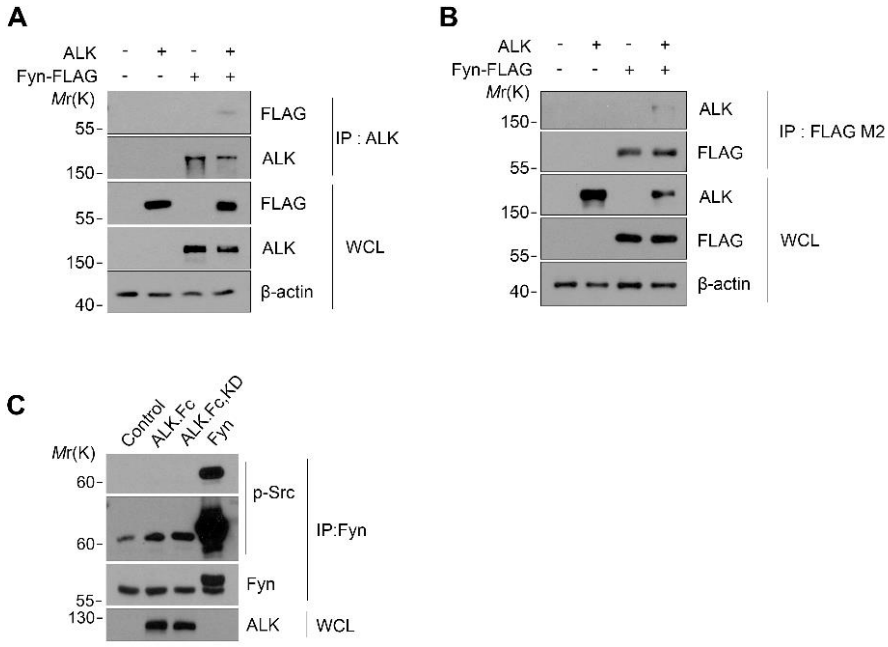
A
ALK - + - +
Fyn-FLAG - - + +
Mr(K)
55-
150-
55-
150-
40-
FLAG
ALK
FLAG
ALK
β-actin
IP : ALK
WCL
B
ALK - + - +
Fyn-FLAG - - + +
Mr(K)
150-
55-
150-
55-
40-
ALK
FLAG
ALK
FLAG
β-actin
IP : FLAG M2
WCL
C
Control
ALK.Fc
ALK.Fc,KD
Fyn
Mr(K)
60-
60-
55-
130-
p-Src
Fyn
ALK
IP:Fyn
WCL

Figure I-16. A dominant-negative form of Grb2 (SH2 DN) attenuates ALK-induced tau accumulation and autophagosomal dysfunction.

(A) SH-SY5Y cells stably expressing ALK and GFP-tau were transfected for 24 h with control vector (-), GRB10, PLCG1 or GRB2 SH2-DN. (B) SH-SY5Y/control and SH-SY5Y/ALK stable cells were transfected with BFP-Stx17, RFP-LC3 and control vector (-) or GRB2 SH2-DN. The percentages of GFP-positive RFP-LC3 dots among total LC3 dots (matured autophagosomes) were determined ($n > 30$). Bars depict means ± S.E.M. $^{**}P < 0.01$; one-way ANOVA followed by *Tukey's* test. (C) Grb2 interacts with ALK. SH-SY5Y cells were transfected for 24 h with Grb2-FLAG or ALK or both for 48 h, Grb2-FLAG was immunoprecipitated (IP) with FLAG-M2 beads, and the immune complexes were assessed by Western blot (WB) with the antibody to ALK.

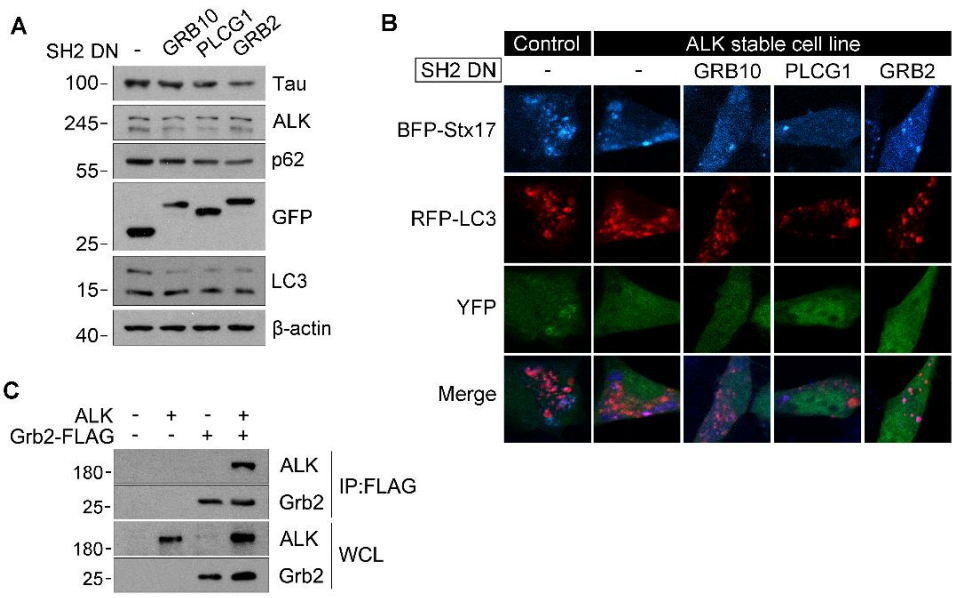
A
SH2 DN
-
GRB10
PLCG1
GRB2
100-
245-
55-
25-
15-
40-
Tau
ALK
p62
GFP
LC3
β-actin
B
Control
ALK stable cell line
SH2 DN
-
-
GRB10
PLCG1
GRB2
BFP-Stx17
RFP-LC3
YFP
Merge
C
ALK
Grb2-FLAG
180-
25-
180-
25-
ALK
Grb2
ALK
Grb2
IP:FLAG
WCL

Figure I-17. ALK causes axonal swelling and spine loss.

(A) ALK induces axonal swelling in primary neurons. Primary cortical neurons (DIV8) were transfected for 24 h with RFP-LC3 plus control vector, ALK.Fc or ALK.Fc.KD, and observed under a confocal microscope (left). The numbers of neurons with LC3-positive swollen axons were counted ($n >$ 60) (right). Bars depict means ± S.E.M. ***$P < 0.001$; one-way ANOVA followed by *Tukey's* test. **(B)** An agonistic ALK antibody reduces spine density on primary neurons. Mouse hippocampal neurons (DIV 13) were transfected with GFP for 2 days and then incubated for an additional 12 h with control immunoglobulin G (IgG) or an agonistic (mAb46) or antagonistic (mAb30) monoclonal ALK antibody in the absence or presence of the ALK inhibitors PF-02341066 (PF, 100 nM) and NVP-TAE684 (TAE, 100 nM). Spine dendrites on the neurons were examined under a fluorescence microscope.

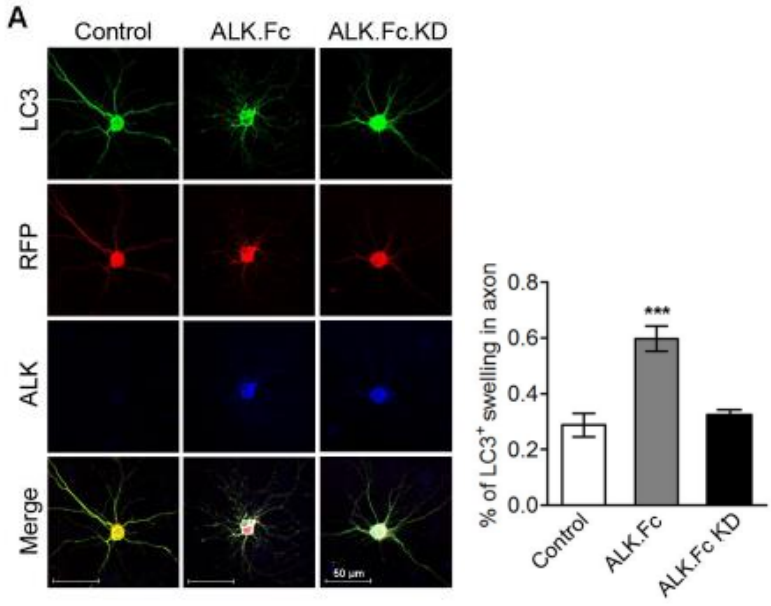
A
Control
ALK.Fc
ALK.Fc.KD
LC3
RFP
ALK
Merge
50 µm
% of LC3+ swelling in axon
0.8
0.6
0.4
0.2
0.0
***
Control
ALK.Fc
ALK.Fc KD

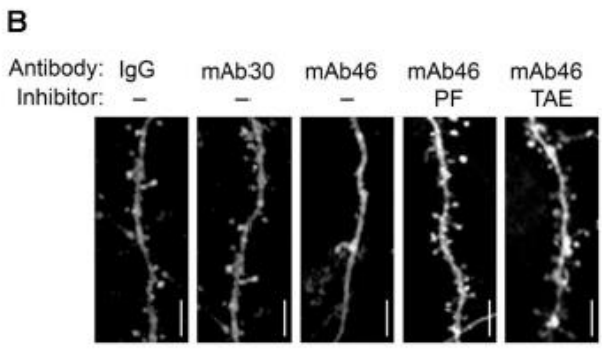
B
Antibody: IgG mAb30 mAb46 mAb46 mAb46
Inhibitor: – – – PF TAE

Figure I-18. ALK leads to neuronal cell death.

(A) Agonistic ALK antibody increases death among primary neurons. Mouse hippocampal neurons (DIV13) were transfected with GFP for 2 days and then incubated with immunoglobulin G (IgG), mAb46 or mAb30 antibody for 12 h. Cell viability was determined using ethidium homodimer ($n > 4$). *$P < 0.05$; Bonferroni *t*-test. Bars depict means value ± S.D. (B) A dominant-negative form of Grb2 (SH2 DN) attenuates ALK-induced cell death. HT22 cells were cotransfected for 48 h with GFP-tau or ALK plus control vector or dominant negative form of Grb2 for 48 h. The apoptosis of GFP-positive cells was analyzed by propidium iodide staining under fluorescence microscope. Bars depict means ± S.E.M. **$P < 0.01$; one-way ANOVA followed by Tukey's test.

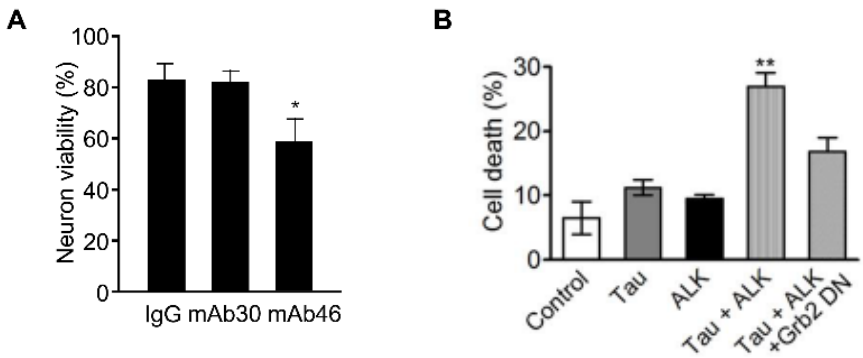
A
Neuron viability (%)
100
80
60
40
20
0
*
IgG mAb30 mAb46
B
Cell death (%)
30
20
10
0
**
Control
Tau
ALK
Tau + ALK
Tau + ALK +Grb2 DN

Figure I-19. ALK is upregulated in AD brains.

(A) Increased expression of ALK in AD brains. Hippocampal lysates from normal elderly controls and patients with AD were analyzed by western blotting (left). Total ALK levels were quantified and normalized to β-actin (right). Bars depict means ± S.E.M; unpaired two-tailed *t*-test. (B) Colocalization of ALK and p-tau within the cortex of AD patients. Hippocampal tissue.

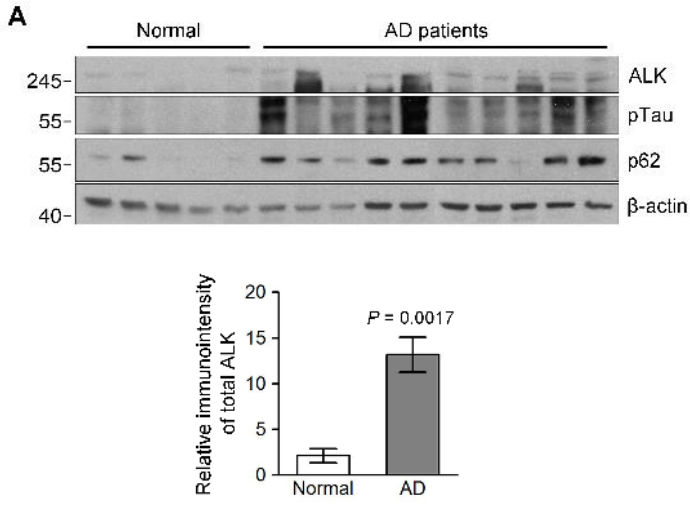
A
Normal
AD patients
245-
55-
55-
40-
ALK
pTau
p62
β-actin
Relative immunointensity of total ALK
20
15
10
5
0
P = 0.0017
Normal
AD

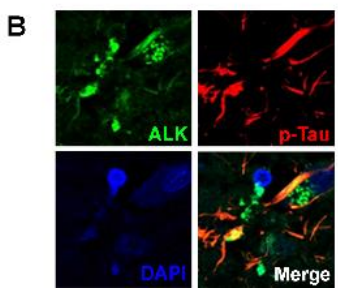
B
ALK
p-Tau
DAPI
Merge

Figure I-20. ALK exacerbates memory deficits in 3xTg-AD mice.

(A-C) Lentiviral delivery of ALK exacerbates memory impairment in 3xTg-AD mice. Lentivirus carrying control (Ctrl) or ALK.Fc (ALK.Fc) was stereotaxically injected into the dentate gyrus of 4- to 5-month-old wild-type (WT) and 3xTg-AD mice. After 30 days, Y-maze (A), passive avoidance (B) and novel object recognition (C) tests were performed. Bars depict means ± SEM; Student's *t*-test. (D) ALK increases abnormal tau phosphorylation in 3xTg-AD mice. Brain extracts from the mice were analyzed by western blotting. Levels of tau phosphorylation in the transgenic mice were analyzed by western blotting, and lentiviral delivery of ALK was confirmed using a Venus antibody.

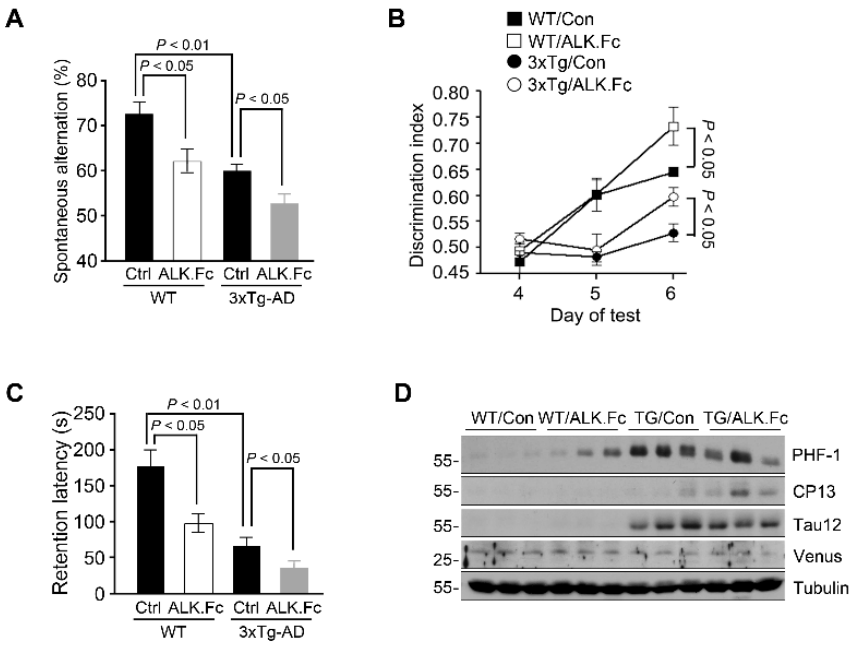
A
P < 0.01
P < 0.05
P < 0.05
Spontaneous alternation (%)
80
70
60
50
40
Ctrl ALK.Fc Ctrl ALK.Fc
WT
3xTg-AD
B
WT/Con
WT/ALK.Fc
3xTg/Con
3xTg/ALK.Fc
Discrimination index
0.80
0.75
0.70
0.65
0.60
0.55
0.50
0.45
P < 0.05
P < 0.05
4
5
6
Day of test
C
P < 0.01
P < 0.05
P < 0.05
Retention latency (s)
250
200
150
100
50
0
Ctrl ALK.Fc Ctrl ALK.Fc
WT
3xTg-AD
D
WT/Con WT/ALK.Fc TG/Con TG/ALK.Fc
55-
PHF-1
55-
CP13
55-
Tau12
25-
Venus
55-
Tubulin

Figure I-21. Pharmacological inhibition of ALK inhibits tau phosphorylation and memory impairments.

(A-C) Intracerebroventricular injection of PF-2341066 ameliorates memory deficits in TauC3 mice. One-month-old TauC3 and age-matched wild-type (WT) mice were administered 9 mg PF-2341066 or DMSO (Mock) via intracerebroventricular injection (n = 6-8). After 3-4 weeks, Y-maze (A), novel object recognition (B) and passive avoidance (C) tests were performed. Bars depict means ± SEM; Student's t-test. (D) ALK inhibition reduces levels of phosphorylated tau in TauC3 mice. Brain extracts from the mice were analyzed by western blotting.

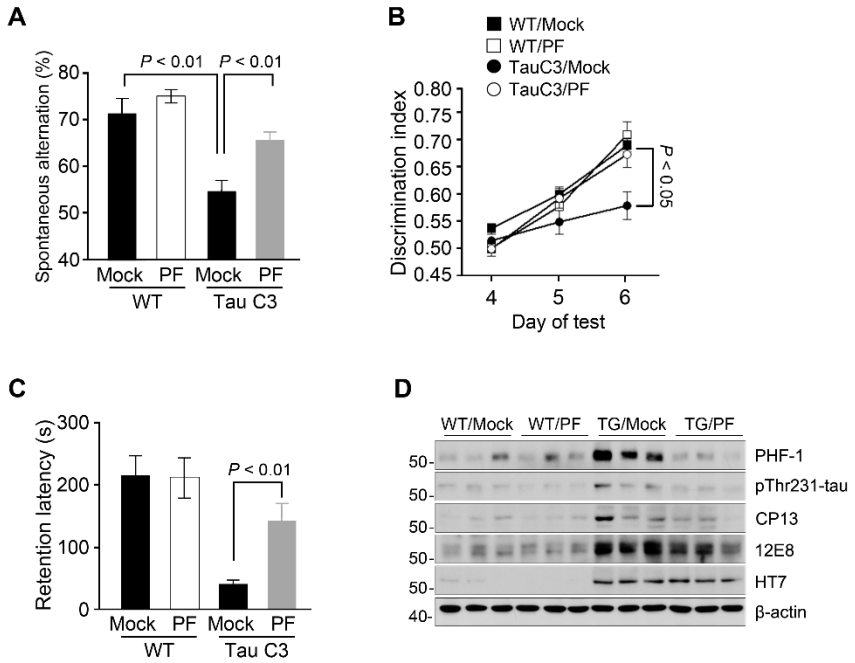
A
Spontaneous alternation (%)
80
70
60
50
40
P < 0.01
P < 0.01
Mock
PF
Mock
PF
WT
Tau C3
B
WT/Mock
WT/PF
TauC3/Mock
TauC3/PF
Discrimination index
0.80
0.75
0.70
0.65
0.60
0.55
0.50
0.45
P < 0.05
4
5
6
Day of test
C
Retention latency (s)
300
200
100
0
P < 0.01
Mock
PF
Mock
PF
WT
Tau C3
D
WT/Mock
WT/PF
TG/Mock
TG/PF
50-
50-
50-
50-
50-
40-
PHF-1
pThr231-tau
CP13
12E8
HT7
β-actin

Figure I-22. LDK378, an ALK inhibitor, is able to mitigate ALK-mediated autophagy impairment and tau accumulation.

SH-SY5Y cells were cotransfected for 24 h with 125 ng of GFP-tau and 250 ng of control vector or ALK.Fc and then treated with different dose of Ceritinib (0.01, 0.1, 1 μM each). After 24 h, cell lysates were subjected to Western blot analysis with indicated antibodies.

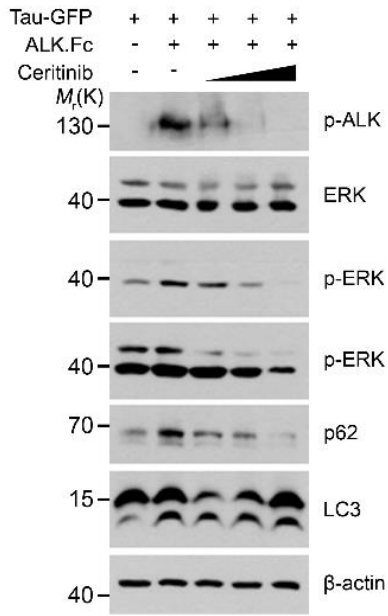
Tau-GFP + + + + +
ALK.Fc - + + + +
Ceritinib - -
M_r(K)
130
p-ALK
40
ERK
40
p-ERK
40
p-ERK
70
p62
15
LC3
40
β-actin

Figure I-23. Pharmacological inhibition of ALK rescues memory impairment in 3xTg-AD mice.

(A-C) LDK378 rescues memory in 3xTg-AD mice. Six-month-old 3xTg-AD mice were intraperitoneally injected with 5 mg/kg LDK378 or DMSO (Mock) (n = 7- 8) daily for 4 weeks and then analyzed using Y-maze (A), novel object recognition (B) and passive avoidance (C) tests. (D, E) Intraperitoneally injected LDK378 reduces tau phosphorylation and accumulation in the brains of 3xTg-AD mice. Hippocampal extracts from the mice were examined by western blotting. Levels of total tau (TG5), exogenous human tau (HT7), phosphorylated tau (PHF1, CP13), p-ERK and ERK on the blots were quantified and normalized to β-actin. Bars depict means ± S.E.M. $^{**}P < 0.01$, $^{***}P < 0.001$; one-way ANOVA followed by Tukey's test.

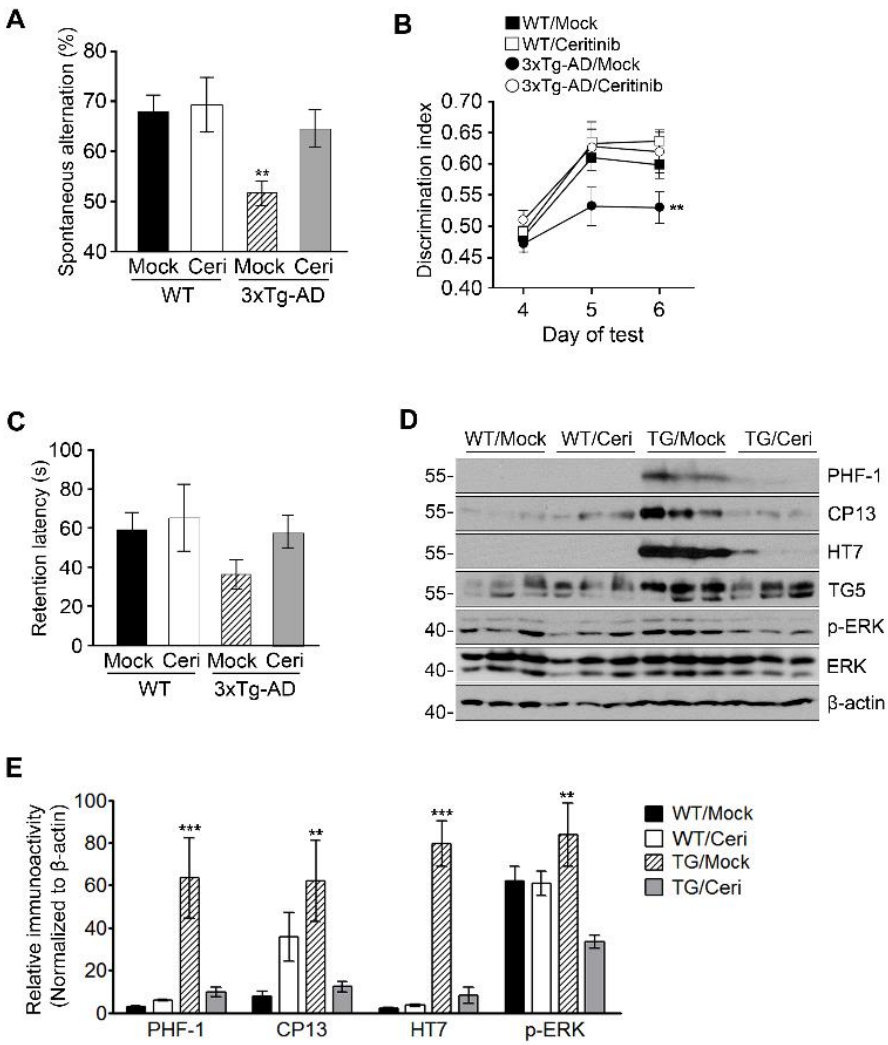
A
Spontaneous alternation (%)
80
70
60
50
40
**
Mock Ceri Mock Ceri
WT
3xTg-AD
B
WT/Mock
WT/Ceritinib
3xTg-AD/Mock
3xTg-AD/Ceritinib
Discrimination index
0.70
0.65
0.60
0.55
0.50
0.45
0.40
**
4 5 6
Day of test
C
Retention latency (s)
100
80
60
40
20
0
Mock Ceri Mock Ceri
WT
3xTg-AD
D
WT/Mock WT/Ceri TG/Mock TG/Ceri
55-
55-
55-
55-
40-
40-
40-
PHF-1
CP13
HT7
TG5
p-ERK
ERK
β-actin
E
Relative immunoactivity
(Normalized to β-actin)
100
80
60
40
20
0
***
**
***
**
PHF-1
CP13
HT7
p-ERK
WT/Mock
WT/Ceri
TG/Mock
TG/Ceri

Figure I-24. Proposed role of ALK in tau-mediated neurotoxicity and memory impairment in AD.

Aberrantly activated ALK is a bona fide mediator of a proteinopathy that disrupts autophagosome maturation and causes tau accumulation, leading to neuronal dysfunction in AD.

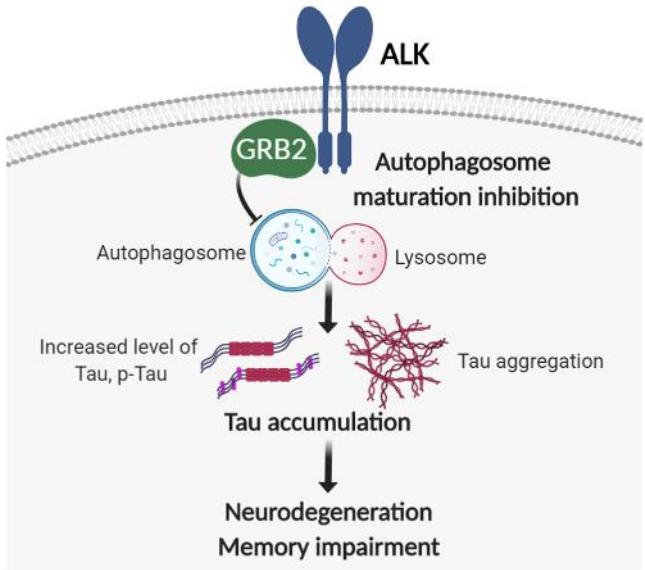
ALK
GRB2
Autophagosome
maturation inhibition
Autophagosome
Lysosome
Increased level of
Tau, p-Tau
Tau aggregation
Tau accumulation
Neurodegeneration
Memory impairment

Discussion

Up to now, genome-wide functional screening for mediators regulating the pathogenesis of tauopathies has achieved only limited success. We therefore established a cell-based tau aggregation assay using TauC3-GFP. TauC3 is generated under stress conditions and is found in the brains of AD patients (Gamblin et al., 2003). TauC3 aggregates faster than wild-type tau *in vitro* (Gamblin et al. 2003) and is localized within tau aggregates in P301S, rTG4510 and TauC3 mice (Zhang, Zhang and Sun 2009; Delobel et al. 2008; de Calignon et al. 2010). To identify a regulator that affects tau aggregation, we utilized TauC3-GFP aggregation assays and screened a cDNA library encoding thousands of membrane proteins. We employed gain-of-function screening using cDNA over loss-of-function screening using siRNA or sgRNA because the latter may not effectively identify a regulator if the signal is not operating. Overexpressed ALK was activated through autophosphorylation as expected (Iwahara et al. 1997; Loren et al. 2001) and affected tau aggregation.

Within the brain, ALK is highly expressed from the embryo stage through postnatal day 7, and a minimum level is maintained into adulthood (Bilsland et al. 2008). It is noteworthy that ALK is up-regulated in the brains of patients with AD and its sustained activation in postmitotic neurons in flies

and cultured differentiated neurons leads to deteriorating changes in those neurons. In general, it is known that ALK mainly functions in neural differentiation during development and aberrant activation of ALK as a consequence of the genetic mutation stimulates cell proliferation, providing a driving force for tumorigenesis in peripheral tissue. In our model, the persistent pressure caused by ALK activation in postmitotic neurons may be a risk factor for pathophysiological processes through tau regulation. This would be analogous to what is observed with histone deacetylase (HDAC), inhibitors of which show promise as anticancer agents and for the prevention of neuronal loss (Kazantsev and Thompson 2008; Bolden, Peart, and Johnstone 2006).

Alk knockout mice have full-life span and show no obvious tissue abnormalities. Two conflicting studies reported about the role of ALK in hippocampal neurogenesis and the behavioral task of *Alk* knockout mice (Bilsland et al. 2008; Weiss et al. 2012). In addition, it was shown that ALK mediates maturation of the newborn neuron via pleiotrophin secreted by adult neuron stem cells (Tang et al. 2019), and regulates amplitude of spontaneous excitatory post-synaptic currents and GABA transmission in the affected neurons (Mangieri et al. 2017; Schweitzer et al. 2016). Similarly, *C. elegans* ALK was proposed to destabilize presynaptic differentiation, while loss of *D. melanogaster* ALK results in the failure of normal midgut development (Liao

et al. 2004; Lee et al. 2003; Englund et al. 2003). Inhibition of dALK in adult α/β mushroom body neurons promotes long-term memory formation, whereas its overexpression impairs it (Gouzi et al. 2018). Thus, the functions of ALK in the brain might depend on brain regions, neuron types, maturation stages of neurons as well as the strength of ALK signaling, which needs to clarify more in the future. We here demonstrated the pathogenic role of ALK in mature primary neurons and 7 to 8 month-old mice.

A few studies have previously reported tau regulators, including mTORC1, Nuak1, and Fyn (Kim et al. 2014; Lasagna-Reeves et al. 2016; Li and Gotz 2017). Fyn, in particular, is known to promote translation and somatodendritic localization of tau in neurons (Li and Gotz 2017). We also observed that overexpressed Fyn interacts with ALK and that Fyn inhibitors, PP1 and PP2 targeting several members of the Src-family (Lee et al. 2004), partially reversed the effect of ALK on tau accumulation. However, we could not assure evidence showing the regulation of Fyn and mTORC1 by ALK in tau accumulation.

Materials and methods

Cell culture

HT22 and SH-SY5Y cells were cultured in Dulbecco's Modified Eagles Medium (GE healthcare, Cat# SH30243.01) with 10% (v/v) fetal bovine serum (Thermo Fisher Scientific, Cat# 26140-079). Stably tau-expressing HT22 cells were maintained in media supplemented with 200 µg/ml hygromycin B (Sigma Aldrich, Cat# 31282-04-9) and tau expression was induced by the treatment with 1 µg/ml doxycycline (Sigma Aldrich, Cat# 10592-13-9). Primary mouse hippocampal neurons were cultured at embryonic day 17. Briefly, resected mouse brain hippocampi and cortices were trypsinized with 0.05% Trypsin-EDTA (Thermo Fisher Scientific, Cat# 25300-062) for 20 min and neuronal cells were transferred to neurobasal medium (Thermo Fisher Scientific, Cat# 21103049) containing B27 serum supplement (Thermo Fisher Scientific, Cat# 17504044) and seeded on twelve-well tissue culture plates at a density of $2x10^6$ cells per well.

Generation of tau stable cell line

HT22 cells were transfected with pBIG2i-tau for 36 h and then cultivated in selection medium containing 200 µg/ml hygromycin B (Sigma Aldrich, Cat# 31282-04-9) for 2 weeks. A single cell was further cultivated to form stable

cell clones, and the expression level of each was analyzed by western blotting in the presence of doxycycline (Sigma Aldrich, Cat# 10592-13-9). SH-SY5Y cells were transfected with GFP-Tau and cultivated in media supplemented with 1 mg/ml G418 (Gold Biotechnology, Cat# G-418-5) for 2 weeks to generate a mixed cell population. A single cell was grown to form a stable cell line.

Drosophila

The gl-Tau2.1 line expressing wild-type human tau4R in pExpress-gl modification of the GMR expression vector and showing a moderate phenotype on the third chormosome was obtained from Dr. Daniel Geschwind (University of California-Los Angeles, CA) (Jackson et al. 2002). UAS-Tau fly line for the generation of elav-tau was obtained from Dr. Mel Feany (Wittmann et al. 2001). The wild-type full-length drosophila ALK fly line, UAS-dALKFL, and drosophila ALK mutants fly lines, UAS-dALKACT and UAS-dALKDN, were generously provided from Dr. Ruth Palmer (The Salk Institute, CA) and Dr. Manfred Frasch (Mount Sinai School of Medicine, NY), respectively (Lee et al. 2003; Loren et al. 2001; Loren et al. 2003). The constitutively active ALK encodes a fusion construct of codons 1-117 of human nucleophosmin (NPM) and codons 1129-1701 of drosophila ALK. The dominant-negative ALK construct encodes the extracellular domain,

transmembrane domain and a short tail of the intracellular domain of drosophila ALK. Flies were grown on standard cornmeal-based drosophila media at 25 °C. Adult flies were used for analysis 5 days posteclosion.

Mice

WT (C57BL/6), TauC3, 3xTg-AD, and ALK -/- mice were used. TauC3 mice were produced as previously described (Kim, Choi, et al. 2016). The ALK -/- mice were gifts from R. Palmer (University of Gothenburg, Gothenburg, Sweden). Mice were raised under a 12 : 12 h light-dark cycle with free access to food and water *ad libitum*. For primary cortical and hippocampal neuron culture, pregnant females and its embryos were sacrified betwenn TP16-TP17. All experiments involving animals were performed according to the protocols approved by the Seoul National University Institutional Animal Care and Use Committee (SNU IACUC) guidelines.

Construction of plasmids

Tau (2N4R), the human longest form, in mammalian expression pCI vector was provided by Dr. Akihiko Takashima (RIKEN, Japan). Tau cDNA was subcloned into pcDNA3-HA (Invitrogen), pGFP (Clontech) and pBIG2i containing the tetracycline-regulated promoter for regulating the expression of an inserted gene and the selection marker for hygromycin B to generate

HA or GFP fusion protein (pHA-tau, pGFP-tau, and pBIG2i-tau, respectively) (Krishnamurthy and Johnson 2004). Mouse ALK in mammalian expression pME18S-FL3 (pmALK) was obtained from Dr. Tadashi Yamamoto (University of Tokyo, Japan) (Iwahara et al., 1997). Full-length human ALK (ALK) and kinase-dead mutant (ALK KD; originally named ALKΔATP) in which the invariant lysine residue (K1150) located in the ATP-binding region was mutated to alanine were provided by Dr. Anton Wellstein (Georgetown University, DC) (Kuo et al. 2007) and subcloned into pcDNA3.1/Myc-His (pALK and pALK KD, respectively). ALK chimera (ALK.Fc) containing mouse IgG 2b Fc domain instead of the extracellular domain of the receptor in pcDNA3.1 and its kinase-defective form (ALK.Fc KD; originally named ALK*.Fc) in pcDNA3.1 (pALK.Fc and pALK.Fc KD, respectively) were gifts from was a gift from Dr. Mel Vigny (INSERM U440, Paris) (Souttou et al. 2001). ALK.Fc and ALK.Fc KD were subcloned into lentiviral pCSII-EF-MCS-IRES2-Venus vector for the production of lentivirus (pLenti-ALK.Fc and pLenti-ALK.Fc KD, respectively).

Transfection, cell death assessment, and viability assay

Expression plasmids were transfected using Lipofectamine 2000 (Invitrogen) or Lipofector-pMax (Aptabio) following the manufacturer's instructions. Cells were stained with 2 μg/ml P.I. for 5 min or 3 μg/ml ethidium homodimer

(EtHD; Molecular Probes) for 10 min. Cell death was assessed by counting cells with condensed, or fragmented nuclei or EtHD18-positive cells.

Preparation of human brain samples and ethical statement

Anterior hippocampal tissues were a kind gift from the Harvard Brain Tissue Resource Center (McLean Hospital). The mean age and post-mortem interval of AD patients (Braak V-VI) was 82.5 +/- 10.8 years (mean +/- SD) and 22 +/- 5.4 h (mean +/- SD) respectively; 66.6% were female. The mean age and post-mortem interval of non-AD patients was 52.25 +/- 9.94 years (mean +/- SD) and 16.3 +/- 7.3 h (mean +/- SD) respectively; 60% were female. Hippocampal tissues of AD patients and controls were lysed in ice-cold Tris-buffered saline (TBS) buffer [20 mM Tris-Cl (pH 7.4), 150 mM NaCl and protease inhibitor cocktails] and then the lysates were centrifuged at 13,000 rpm for 20 min at 4 °C. The supernatants were subjected to SDS-PAGE. This study was approved by the Institutional Review Board of Seoul National University.

Preparation of tissue lysates from mouse brain and fly heads

Tissue regions of brain were homogenized in Tris-buffered saline [TBS; 20 mM Tris-Cl (pH 7.4), 150 mM NaCl, 1% Triton X-100, 1 mM Na_3VO_4, 1 mM NaF, 1 mM PMSF and 1 μg/ml each of aprotinin, leupeptin and pepstatin

A]. Fly heads were homogenized in homogenization buffer [50 mM Tris-Cl (pH 8.0), 150 mM NaCl, 1% Triton X-100, 10% sucrose, 1 mM Na_3VO_4, 1 mM NaF, 1 mM PMSF and 1 μg/ml each of aprotinin, leupeptin and pepstatin A]. The homogenates were centrifuged at 15,000 *g* for 30 min and protein concentrations in resultant supernatants were determined using Bradford assay (Bio-Rad).

Western blot analysis

Cells were lysed in ice-cold RIPA buffer [50 mM Tris-Cl (pH 8.0), 15 mM NaCl, 1% Triton X-100, 0.5% sodium deoxycholate, 0.1% SDS, 1 mM PMSF and 1 μg/ml each of aprotinin, leupeptin and pepstatin A]. For ALK protein detection, cell lysates were incubated at 37 °C for 15 min after lysis. Cell lysates were clarified by centrifugation at 13,000*g* for 10 min, diluted in 2× SDS loading buffer [100 mM Tris-Cl (pH 6.8), 4% SDS, 20% glycerol, 0.01% bromophenol blue, and 10% β-mercaptoethanol], resolved by SDS-PAGE and transferred onto PVDF membrane.

Antibodies

The following anti-tau antibodies were used: DA9 (total Tau; generously provided by Dr. Peter Davies, Albert Einstein College of Medicine, NY), phospho-Tau Ser396 (Invitrogen, Cat# 44-752G), LC3 (Novus Biologicals,

Cat# NB600-1384), anti-SQSTM1 (Abnova, Cat# H00008878-M01), p-ALK (p-Tyr1604; Cell signaling, Cat# 3341), ALK1 (BD Pharmingen, Cat# 559254), ALK (Invitrogen, Cat# 51-3900), ALK (DAKO, Cat# IS64130-2), β-actin (Sigma Aldrich, Cat# A2668) and GFP (Santa Cruz, Cat# sc-8334).

Immunocytochemistry

Cells were fixed with 4% paraformaldehyde for 15 min and then permeabilized with 0.1% Triton X-100 for 15 min, followed by blocking with 4% BSA. Primary antibody staining with DA9, phospho-Tau Ser396 (Invitrogen, Cat# 44-752G), ALK (Thermo Scientific, MA5-14528) and ALK (DAKO, Cat# IS64130-2) were applied for total tau, pTau, ALK detection. Between steps, there are 3 times wash with 1X PBS. Images were obtained with 40X objective by using a confocal laser scanning microscope (Carl Zeiss, LSM700)

Immunohistochemistry of human brain tissue

Human brain tissues were provided by Brain Bank of Seoul National University Hospital Biomedical Research Institute. Hippocampal sections from AD patients were retrieved with 10% formic acid for 15 min at 37 °C and then blocked with 5% BSA. Blocked sections were stained with antibodies against ALK (DAKO, Cat# IS64130-2) and pTau S386 pTau S386

(Invitrogen, Cat# 44-752G) at 4 °C overnight to detect human ALK and neurofibrillary tangles, respectively. Anti-rabbit Alexa Fluor 488 (Molecular Probes, Cat# A11008) and anti-mouse Alexa Fluor 594 (Molecular Probes, Cat# A11005) were applied at R.T. for 1 h as secondary antibody. Slides were stained with Hoechst 33342 (Molecular Probes, Cat# H3570) at R.T. for 5 min and mounted with mounting medium (Sigma Aldrich, Cat# F4680) and images obtained with 40X objective by a confocal laser scanning microscope (Carl Zeiss, LSM700)

Lentivirus production

Lentiviral vector stock was produced in HEK 293FT cells following calcium phosphate-mediated transfection of the modified transfer vector, packing vectors pMDLg/pRRE and pCMV-VSV-G-RSV-Rev. Supernatants were harvested over 48 to 60 h and concentrated by ultracentrifugation at 50,000 *g* for 2 h at 4 °C. Virus titers were assessed by transducing HEK 293 cells with serial dilutions of viral stock.

Stereotaxic injection

Lentivirus expressing CSII-EF-MCS-IRES2-Venus-ALK.Fc and control virus were used for injection. The lentivirus (2.27 x 10^9 TU/ml, TU; transduction unit) was stereotaxically injected bilaterally into the dentate

gyrus (2 µl per hemisphere at 0.4 µl/min). We use the following coordinates to target the DG: anteroposterior = 2.1 mm from bregma, mediolateral = ± 1.8 mm, dorsoventral = 2.0 mm.

Behavior tests

Y Maze Spontaneous Alternation Test. The mice were placed at the end of one arm and allowed to explore freely through the maze (32.5 cm length x 15 cm height) for 7 min. An entry occurs when all 4 paws are placed into the arm. The number of arm entries and the number of total alterations were recorded and calculated for the percentage. After each trial, the apparatus was cleaned with 70% ethanol.

2-Novel object recognition. During the habituation, the mice were allowed to move within an empty white plastic chamber (22 cm wide × 27 cm long × 30 cm high) for 7 min at 24-hour intervals. After 2 days, the mice were exposed to 2 objects and allowed to explore freely for 7 min. In the testing trial performed 24 h later, 1 of the familiar objects was replaced with a novel object and the time spent exploring each object was recorded during a 7-minute period. Between each trial, the arena and objects were wiped down with 70% ethanol.

Passive avoidance Task. The passive avoidance chamber is divided into a light compartment and a dark compartment (20 × 20 × 20 cm each) separated by a guillotine door. During the habituation, mice were allowed to freely explore both compartments for 5 min. On the following day, electric foot shock (0.25 mA, 2 seconds) was delivered to the mice were when both hindlimbs of the mice were entered into the dark box. For the test, mice were placed back in the light box 24 h after the conditioning. The latency time for the mice to enter the dark compartment was measured with a 7-minute cut-off point.

Quantification and statistical analysis

Statistical analyses were conducted using Prism. Data are expressed as mean ± S.E.M. Statistical comparisons between two groups were performed using two-tailed t-test and comparisons between multiple groups were performed using one-way analysis of variance (ANOVA) followed by Tukey's test as appropriate.

References

Bemiller, S. M., T. J. McCray, K. Allan, S. V. Formica, G. Xu, G. Wilson, O. N. Kokiko-Cochran, S. D. Crish, C. A. Lasagna-Reeves, R. M. Ransohoff, G. E. Landreth, and B. T. Lamb. 2017. 'TREM2 deficiency exacerbates tau pathology through dysregulated kinase signaling in a mouse model of tauopathy', *Mol Neurodegener*, 12: 74.

Bergeron, C., M. S. Pollanen, L. Weyer, and A. E. Lang. 1997. 'Cortical degeneration in progressive supranuclear palsy. A comparison with cortical-basal ganglionic degeneration', *J Neuropathol Exp Neurol*, 56: 726-34.

Bilsland, J. G., A. Wheeldon, A. Mead, P. Znamenskiy, S. Almond, K. A. Waters, M. Thakur, V. Beaumont, T. P. Bonnert, R. Heavens, P. Whiting, G. McAllister, and I. Munoz-Sanjuan. 2008. 'Behavioral and neurochemical alterations in mice deficient in anaplastic lymphoma kinase suggest therapeutic potential for psychiatric indications', *Neuropsychopharmacology*, 33: 685-700.

Bolden, Jessica E., Melissa J. Peart, and Ricky W. Johnstone. 2006. 'Anticancer activities of histone deacetylase inhibitors', *Nat Rev Drug Discov*, 5: 769-84.

Brand, A. H., and N. Perrimon. 1993. 'Targeted gene expression as a means

of altering cell fates and generating dominant phenotypes', *Development*, 118: 401-15.

Bugiani, O., J. R. Murrell, G. Giaccone, M. Hasegawa, G. Ghigo, M. Tabaton, M. Morbin, A. Primavera, F. Carella, C. Solaro, M. Grisoli, M. Savoiardo, M. G. Spillantini, F. Tagliavini, M. Goedert, and B. Ghetti. 1999. 'Frontotemporal dementia and corticobasal degeneration in a family with a P301S mutation in tau', *J Neuropathol Exp Neurol*, 58: 667-77.

Busche, M. A., S. Wegmann, S. Dujardin, C. Commins, J. Schiantarelli, N. Klickstein, T. V. Kamath, G. A. Carlson, I. Nelken, and B. T. Hyman. 2019. 'Tau impairs neural circuits, dominating amyloid-beta effects, in Alzheimer models in vivo', *Nat Neurosci*, 22: 57-64.

Chen, D., W. Fan, Y. Lu, X. Ding, S. Chen, and Q. Zhong. 2012. 'A mammalian autophagosome maturation mechanism mediated by TECPR1 and the Atg12-Atg5 conjugate', *Mol Cell*, 45: 629-41.

Chen, Y., J. Takita, Y. L. Choi, M. Kato, M. Ohira, M. Sanada, L. Wang, M. Soda, A. Kikuchi, T. Igarashi, A. Nakagawara, Y. Hayashi, H. Mano, and S. Ogawa. 2008. 'Oncogenic mutations of ALK kinase in neuroblastoma', *Nature*, 455: 971-4.

Childress, Merrida A, Abha Gupta, Doron Lipson, Geoff Otto, Tina Brennan, Catherine T Chung, Scott C Borinstein, Jeffrey S Ross, Phillip J

Stephens, and Vincent A Miller. 2015. 'Understanding oncogenic fusions: Lessons learned from inflammatory myofibroblastic tumor', *Cancer Research*, 75: 497-97.

Chung, C. W., Y. H. Song, I. K. Kim, W. J. Yoon, B. R. Ryu, D. G. Jo, H. N. Woo, Y. K. Kwon, H. H. Kim, B. J. Gwag, I. H. Mook-Jung, and Y. K. Jung. 2001. 'Proapoptotic effects of tau cleavage product generated by caspase-3', *Neurobiol Dis*, 8: 162-72.

de Calignon, A., L. M. Fox, R. Pitstick, G. A. Carlson, B. J. Bacskai, T. L. Spires-Jones, and B. T. Hyman. 2010. 'Caspase activation precedes and leads to tangles', *Nature*, 464: 1201-4.

Delacourte, A., N. Sergeant, A. Wattez, D. Gauvreau, and Y. Robitaille. 1998. 'Vulnerable neuronal subsets in Alzheimer's and Pick's disease are distinguished by their tau isoform distribution and phosphorylation', *Ann Neurol*, 43: 193-204.

Delobel, P., I. Lavenir, G. Fraser, E. Ingram, M. Holzer, B. Ghetti, M. G. Spillantini, R. A. Crowther, and M. Goedert. 2008. 'Analysis of tau phosphorylation and truncation in a mouse model of human tauopathy', *American Journal of Pathology*, 172: 123-31.

Egan, D. F., D. B. Shackelford, M. M. Mihaylova, S. Gelino, R. A. Kohnz, W. Mair, D. S. Vasquez, A. Joshi, D. M. Gwinn, R. Taylor, J. M. Asara, J. Fitzpatrick, A. Dillin, B. Viollet, M. Kundu, M. Hansen, and R. J.

Shaw. 2011. 'Phosphorylation of ULK1 (hATG1) by AMP-activated protein kinase connects energy sensing to mitophagy', *Science*, 331: 456-61.

Galkin, A. V., J. S. Melnick, S. Kim, T. L. Hood, N. Li, L. Li, G. Xia, R. Steensma, G. Chopiuk, J. Jiang, Y. Wan, P. Ding, Y. Liu, F. Sun, P. G. Schultz, N. S. Gray, and M. Warmuth. 2007. 'Identification of NVP-TAE684, a potent, selective, and efficacious inhibitor of NPM-ALK', *Proc Natl Acad Sci U S A*, 104: 270-5.

Gamblin, T. C., F. Chen, A. Zambrano, A. Abraha, S. Lagalwar, A. L. Guillozet, M. Lu, Y. Fu, F. Garcia-Sierra, N. LaPointe, R. Miller, R. W. Berry, L. I. Binder, and V. L. Cryns. 2003. 'Caspase cleavage of tau: linking amyloid and neurofibrillary tangles in Alzheimer's disease', *Proc Natl Acad Sci U S A*, 100: 10032-7.

George, R. E., T. Sanda, M. Hanna, S. Frohling, W. Luther, 2nd, J. Zhang, Y. Ahn, W. Zhou, W. B. London, P. McGrady, L. Xue, S. Zozulya, V. E. Gregor, T. R. Webb, N. S. Gray, D. G. Gilliland, L. Diller, H. Greulich, S. W. Morris, M. Meyerson, and A. T. Look. 2008. 'Activating mutations in ALK provide a therapeutic target in neuroblastoma', *Nature*, 455: 975-8.

Guan, J., G. Umapathy, Y. Yamazaki, G. Wolfstetter, P. Mendoza, K. Pfeifer, A. Mohammed, F. Hugosson, H. Zhang, A. W. Hsu, R. Halenbeck, B.

Hallberg, and R. H. Palmer. 2015. 'FAM150A and FAM150B are activating ligands for anaplastic lymphoma kinase', *Elife*, 4: e09811.

Guo, T., W. Noble, and D. P. Hanger. 2017. 'Roles of tau protein in health and disease', *Acta Neuropathol*, 133: 665-704.

Hapgood, Greg, and Kerry J Savage. 2015. 'The biology and management of systemic anaplastic large cell lymphoma', *Blood*: blood-2014-10-567461.

Itakura, E., C. Kishi-Itakura, and N. Mizushima. 2012. 'The hairpin-type tail-anchored SNARE syntaxin 17 targets to autophagosomes for fusion with endosomes/lysosomes', *Cell*, 151: 1256-69.

Ittner, L. M., and J. Gotz. 2011. 'Amyloid-beta and tau--a toxic pas de deux in Alzheimer's disease', *Nat Rev Neurosci*, 12: 65-72.

Ittner, L. M., Y. D. Ke, F. Delerue, M. Bi, A. Gladbach, J. van Eersel, H. Wolfing, B. C. Chieng, M. J. Christie, I. A. Napier, A. Eckert, M. Staufenbiel, E. Hardeman, and J. Gotz. 2010. 'Dendritic function of tau mediates amyloid-beta toxicity in Alzheimer's disease mouse models', *Cell*, 142: 387-97.

Ivankovic, D., J. Drew, F. Lesept, I. J. White, G. Lopez Domenech, S. A. Tooze, and J. T. Kittler. 2019. 'Axonal autophagosome maturation defect through failure of ATG9A sorting underpins pathology in AP-4 deficiency syndrome', *Autophagy*: 1-17.

Iwahara, T., J. Fujimoto, D. Wen, R. Cupples, N. Bucay, T. Arakawa, S. Mori, B. Ratzkin, and T. Yamamoto. 1997. 'Molecular characterization of ALK, a receptor tyrosine kinase expressed specifically in the nervous system', *Oncogene*, 14: 439-49.

Jackson, G. R., M. Wiedau-Pazos, T. K. Sang, N. Wagle, C. A. Brown, S. Massachi, and D. H. Geschwind. 2002. 'Human wild-type tau interacts with wingless pathway components and produces neurofibrillary pathology in Drosophila', *Neuron*, 34: 509-19.

Kam, T. I., S. Song, Y. Gwon, H. Park, J. J. Yan, I. Im, J. W. Choi, T. Y. Choi, J. Kim, D. K. Song, T. Takai, Y. C. Kim, K. S. Kim, S. Y. Choi, S. Choi, W. L. Klein, J. Yuan, and Y. K. Jung. 2013. 'FcgammaRIIb mediates amyloid-beta neurotoxicity and memory impairment in Alzheimer's disease', *J Clin Invest*, 123: 2791-802.

Kang, R., H. J. Zeh, M. T. Lotze, and D. Tang. 2011. 'The Beclin 1 network regulates autophagy and apoptosis', *Cell Death Differ*, 18: 571-80.

Kazantsev, A. G., and L. M. Thompson. 2008. 'Therapeutic application of histone deacetylase inhibitors for central nervous system disorders', *Nat Rev Drug Discov*, 7: 854-68.

Kim, B. M., M. H. You, C. H. Chen, S. Lee, Y. Hong, Y. Hong, A. Kimchi, X. Z. Zhou, and T. H. Lee. 2014. 'Death-associated protein kinase 1 has a critical role in aberrant tau protein regulation and function', *Cell*

Death Dis, 5: e1237.

Kim, D. W., R. Mehra, D. S. W. Tan, E. Felip, L. Q. M. Chow, D. R. Camidge, J. Vansteenkiste, S. Sharma, T. De Pas, G. J. Riely, B. J. Solomon, J. Wolf, M. Thomas, M. Schuler, G. Liu, A. Santoro, S. Sutradhar, S. Li, T. Szczudlo, A. Yovine, and A. T. Shaw. 2016. 'Activity and safety of ceritinib in patients with ALK-rearranged non-small-cell lung cancer (ASCEND-1): updated results from the multicentre, open-label, phase 1 trial', *Lancet Oncol*, 17: 452-63.

Kim, Y., H. Choi, W. Lee, H. Park, T. I. Kam, S. H. Hong, J. Nah, S. Jung, B. Shin, H. Lee, T. Y. Choi, H. Choo, K. K. Kim, S. Y. Choi, R. Kayed, and Y. K. Jung. 2016. 'Caspase-cleaved tau exhibits rapid memory impairment associated with tau oligomers in a transgenic mouse model', *Neurobiol Dis*, 87: 19-28.

Kim, Y. M., C. H. Jung, M. Seo, E. K. Kim, J. M. Park, S. S. Bae, and D. H. Kim. 2015. 'mTORC1 phosphorylates UVRAG to negatively regulate autophagosome and endosome maturation', *Mol Cell*, 57: 207-18.

Krishnamurthy, P. K., and G. V. Johnson. 2004. 'Mutant (R406W) human tau is hyperphosphorylated and does not efficiently bind microtubules in a neuronal cortical cell model', *J Biol Chem*, 279: 7893-900.

Kruger, U., Y. Wang, S. Kumar, and E. M. Mandelkow. 2012. 'Autophagic degradation of tau in primary neurons and its enhancement by

trehalose', *Neurobiol Aging*, 33: 2291-305.

Kuo, A. H., G. E. Stoica, A. T. Riegel, and A. Wellstein. 2007. 'Recruitment of insulin receptor substrate-1 and activation of NF-kappaB essential for midkine growth signaling through anaplastic lymphoma kinase', *Oncogene*, 26: 859-69.

Lasagna-Reeves, C. A., M. de Haro, S. Hao, J. Park, M. W. Rousseaux, I. Al-Ramahi, P. Jafar-Nejad, L. Vilanova-Velez, L. See, A. De Maio, L. Nitschke, Z. Wu, J. C. Troncoso, T. F. Westbrook, J. Tang, J. Botas, and H. Y. Zoghbi. 2016. 'Reduction of Nuak1 Decreases Tau and Reverses Phenotypes in a Tauopathy Mouse Model', *Neuron*, 92: 407-18.

Lee, G., R. Thangavel, V. M. Sharma, J. M. Litersky, K. Bhaskar, S. M. Fang, L. H. Do, A. Andreadis, G. Van Hoesen, and H. Ksiezak-Reding. 2004. 'Phosphorylation of tau by fyn: implications for Alzheimer's disease', *J Neurosci*, 24: 2304-12.

Lee, H. H., A. Norris, J. B. Weiss, and M. Frasch. 2003. 'Jelly belly protein activates the receptor tyrosine kinase Alk to specify visceral muscle pioneers', *Nature*, 425: 507-12.

Lee, V. M., M. Goedert, and J. Q. Trojanowski. 2001. 'Neurodegenerative tauopathies', *Annu Rev Neurosci*, 24: 1121-59.

Leyns, C. E. G., J. D. Ulrich, M. B. Finn, F. R. Stewart, L. J. Koscal, J.

Remolina Serrano, G. O. Robinson, E. Anderson, M. Colonna, and D. M. Holtzman. 2017. 'TREM2 deficiency attenuates neuroinflammation and protects against neurodegeneration in a mouse model of tauopathy', *Proc Natl Acad Sci U S A*, 114: 11524-29.

Li, C., and J. Gotz. 2017. 'Somatodendritic accumulation of Tau in Alzheimer's disease is promoted by Fyn-mediated local protein translation', *Embo j*, 36: 3120-38.

Liao, E. H., W. Hung, B. Abrams, and M. Zhen. 2004. 'An SCF-like ubiquitin ligase complex that controls presynaptic differentiation', *Nature*, 430: 345-50.

Loren, C. E., A. Scully, C. Grabbe, P. T. Edeen, J. Thomas, M. McKeown, T. Hunter, and R. H. Palmer. 2001. 'Identification and characterization of DAlk: a novel Drosophila melanogaster RTK which drives ERK activation in vivo', *Genes Cells*, 6: 531-44.

Moog-Lutz, C., J. Degoutin, J. Y. Gouzi, Y. Frobert, N. Brunet-de Carvalho, J. Bureau, C. Creminon, and M. Vigny. 2005. 'Activation and inhibition of anaplastic lymphoma kinase receptor tyrosine kinase by monoclonal antibodies and absence of agonist activity of pleiotrophin', *J Biol Chem*, 280: 26039-48.

Morris, S. W., M. N. Kirstein, M. B. Valentine, K. G. Dittmer, D. N. Shapiro, D. L. Saltman, and A. T. Look. 1994. 'Fusion of a kinase gene, ALK,

to a nucleolar protein gene, NPM, in non-Hodgkin's lymphoma', *Science*, 263: 1281-4.

Morris, S. W., C. Naeve, P. Mathew, P. L. James, M. N. Kirstein, X. Cui, and D. P. Witte. 1997. 'ALK, the chromosome 2 gene locus altered by the t(2;5) in non-Hodgkin's lymphoma, encodes a novel neural receptor tyrosine kinase that is highly related to leukocyte tyrosine kinase (LTK)', *Oncogene*, 14: 2175-88.

Motegi, A., J. Fujimoto, M. Kotani, H. Sakuraba, and T. Yamamoto. 2004. 'ALK receptor tyrosine kinase promotes cell growth and neurite outgrowth', *J Cell Sci*, 117: 3319-29.

Murray, P. B., I. Lax, A. Reshetnyak, G. F. Ligon, J. S. Lillquist, E. J. Natoli, Jr., X. Shi, E. Folta-Stogniew, M. Gunel, D. Alvarado, and J. Schlessinger. 2015. 'Heparin is an activating ligand of the orphan receptor tyrosine kinase ALK', *Sci Signal*, 8: ra6.

Piras, A., L. Collin, F. Gruninger, C. Graff, and A. Ronnback. 2016. 'Autophagic and lysosomal defects in human tauopathies: analysis of post-mortem brain from patients with familial Alzheimer disease, corticobasal degeneration and progressive supranuclear palsy', *Acta Neuropathol Commun*, 4: 22.

Reshetnyak, A. V., P. B. Murray, X. Shi, E. S. Mo, J. Mohanty, F. Tome, H. Bai, M. Gunel, I. Lax, and J. Schlessinger. 2015. 'Augmentor alpha

and beta (FAM150) are ligands of the receptor tyrosine kinases ALK and LTK: Hierarchy and specificity of ligand-receptor interactions', *Proc Natl Acad Sci U S A*, 112: 15862-7.

Riera, L., E. Lasorsa, C. Ambrogio, N. Surrenti, C. Voena, and R. Chiarle. 2010. 'Involvement of Grb2 adaptor protein in nucleophosmin-anaplastic lymphoma kinase (NPM-ALK)-mediated signaling and anaplastic large cell lymphoma growth', *J Biol Chem*, 285: 26441-50.

Roberson, E. D., K. Scearce-Levie, J. J. Palop, F. Yan, I. H. Cheng, T. Wu, H. Gerstein, G. Q. Yu, and L. Mucke. 2007. 'Reducing endogenous tau ameliorates amyloid beta-induced deficits in an Alzheimer's disease mouse model', *Science*, 316: 750-4.

Roy, K., O. Chakrabarti, and D. Mukhopadhyay. 2014. 'Interaction of Grb2 SH3 domain with UVRAG in an Alzheimer's disease-like scenario', *Biochem Cell Biol*, 92: 219-25.

Shaw, A. T., D. W. Kim, R. Mehra, D. S. Tan, E. Felip, L. Q. Chow, D. R. Camidge, J. Vansteenkiste, S. Sharma, T. De Pas, G. J. Riely, B. J. Solomon, J. Wolf, M. Thomas, M. Schuler, G. Liu, A. Santoro, Y. Y. Lau, M. Goldwasser, A. L. Boral, and J. A. Engelman. 2014a. 'Ceritinib in ALK-rearranged non-small-cell lung cancer', *N Engl J Med*, 370: 1189-97.

Shaw, Alice T., Dong-Wan Kim, Ranee Mehra, Daniel S.W. Tan, Enriqueta

Felip, Laura Q.M. Chow, D. Ross Camidge, Johan Vansteenkiste, Sunil Sharma, Tommaso De Pas, Gregory J. Riely, Benjamin J. Solomon, Juergen Wolf, Michael Thomas, Martin Schuler, Geoffrey Liu, Armando Santoro, Yvonne Y. Lau, Meredith Goldwasser, Anthony L. Boral, and Jeffrey A. Engelman. 2014b. 'Ceritinib in ALK-Rearranged Non–Small-Cell Lung Cancer', *New England Journal of Medicine*, 370: 1189-97.

Shi, Y., K. Yamada, S. A. Liddelow, S. T. Smith, L. Zhao, W. Luo, R. M. Tsai, S. Spina, L. T. Grinberg, J. C. Rojas, G. Gallardo, K. Wang, J. Roh, G. Robinson, M. B. Finn, H. Jiang, P. M. Sullivan, C. Baufeld, M. W. Wood, C. Sutphen, L. McCue, C. Xiong, J. L. Del-Aguila, J. C. Morris, C. Cruchaga, A. M. Fagan, B. L. Miller, A. L. Boxer, W. W. Seeley, O. Butovsky, B. A. Barres, S. M. Paul, and D. M. Holtzman. 2017. 'ApoE4 markedly exacerbates tau-mediated neurodegeneration in a mouse model of tauopathy', *Nature*, 549: 523-27.

Souttou, B., N. B. Carvalho, D. Raulais, and M. Vigny. 2001. 'Activation of anaplastic lymphoma kinase receptor tyrosine kinase induces neuronal differentiation through the mitogen-activated protein kinase pathway', *J Biol Chem*, 276: 9526-31.

Sterniczuk, Roxanne, Michael C Antle, Frank M LaFerla, and Richard H Dyck. 2010. 'Characterization of the 3xTg-AD mouse model of

Alzheimer's disease: part 2. Behavioral and cognitive changes', *Brain research*, 1348: 149-55.

Vernersson, E., N. K. Khoo, M. L. Henriksson, G. Roos, R. H. Palmer, and B. Hallberg. 2006. 'Characterization of the expression of the ALK receptor tyrosine kinase in mice', *Gene Expr Patterns*, 6: 448-61.

Wagner, M. J., M. M. Stacey, B. A. Liu, and T. Pawson. 2013. 'Molecular mechanisms of SH2- and PTB-domain-containing proteins in receptor tyrosine kinase signaling', *Cold Spring Harb Perspect Biol*, 5: a008987.

Yang, H. L., T. Eriksson, E. Vernersson, M. Vigny, B. Hallberg, and R. H. Palmer. 2007. 'The ligand Jelly Belly (Jeb) activates the Drosophila Alk RTK to drive PC12 cell differentiation, but is unable to activate the mouse ALK RTK', *J Exp Zool B Mol Dev Evol*, 308: 269-82.

Yoshii, S. R., and N. Mizushima. 2017. 'Monitoring and Measuring Autophagy', *Int J Mol Sci*, 18.

Zeng, L., R. Kang, S. Zhu, X. Wang, L. Cao, H. Wang, T. R. Billiar, J. Jiang, and D. Tang. 2017. 'ALK is a therapeutic target for lethal sepsis', *Sci Transl Med*, 9.

Zhang, Q. P., X. G. Zhang, and A. Y. Sun. 2009. 'Truncated tau at D421 is associated with neurodegeneration and tangle formation in the brain of Alzheimer transgenic models', *Acta Neuropathol*, 117: 687-97.

Zou, H. Y., Q. Li, J. H. Lee, M. E. Arango, S. R. McDonnell, S. Yamazaki, T. B. Koudriakova, G. Alton, J. J. Cui, P. P. Kung, M. D. Nambu, G. Los, S. L. Bender, B. Mroczkowski, and J. G. Christensen. 2007. 'An orally available small-molecule inhibitor of c-Met, PF-2341066, exhibits cytoreductive antitumor efficacy through antiproliferative and antiangiogenic mechanisms', *Cancer Res*, 67: 4408-17.

CHAPTER II

Isolation and characterization of ALK inhibitors and Agonistic antibodies

Abstract

Anaplastic lymphoma kinase (ALK) has been massively studied for its role in tumorigenesis. In addition, my previous study demonstrated that ALK is responsible for tau pathology in Alzheimer's disease (AD). Recently, increasing studies reported that ALK also functions in septic conditions by regulating STING pathway. As ALK has been shown to function in many diseases, including cancers and neuronal degenerative diseases, it becomes increasingly important to regulate the activity of ALK. More, it has not been clearly shown on ALK ligand.

Thus, I aimed to find a way to manipulate ALK activity through various tools, including small molecule inhibitors and antibodies. First, I screened 1,568 brain-blood-barrier-penetrating small molecules to isolate ALK inhibitors targeting non-active site. I isolated 5 compounds to inhibit the activity of ALK and the accumulation and aggregation of tau. According to *in vitro* kinase assay and cell-based assays, the compounds are considered to inhibit ALK via targeting non-active site. I also tested the *in vivo* effect of KRCA0605, an ALK inhibitor targeting its active site and found that oral administration of KRCA0605 alleviated memory impairment of 3xTg-AD mice. Accordingly, levels of total tau and phosphorylated tau were reduced by KRCA0605. In addition, I tested putative ALK antibodies isolated from a

phage display antibody library panning and verified their binding to ALK located on cell surface by FACS analysis. Among those antibodies, at least 2 antibodies seem to active ALK and also increase tau accumulation, thus showing agonistic effects to ALK. Collectively, I illustrate new inhibitors and antibodies regulating ALK activity, providing new opportunity for the analysis of pathophysiology and for the treatment options of diseases associated with ALK.

Introduction

Anaplastic lymphoma kinase (ALK) belongs to the insulin receptor superfamily and is exclusively expressed in neurons of the nerve system. ALK comprises an extracellular domain, a single pass transmembrane region, and an intracellular kinase domain. ALK has role in the development of the brain and, more importantly, been studies for its role in tumorigenesis (Iwahara et al. 1997; Motegi et al. 2004). A variety of fusion ALK proteins with NPM, TPM4 (Tropomyosin 4) or EML (Echinoderm Microtubule-Associated Protein-Like) are found in inflammatory myofibroblastic tumors (IMT), non-small-cell lung cancers (NSCLC), anaplastic large-cell lymphoma (ALCL), and other cancers (Morris et al. 1994; Morris et al. 1997). Various ALK mutations are identified in anaplastic thyroid cancer (ATC), NSCLC, IMT, and neuroblastoma (Chen et al. 2008; George et al. 2008). ALK overexpression also has been reported in melanoma, ovarian cancer, breast cancer, and NSCLC (Hallberg and Palmer 2013). Among ALK-positive cancers, NSCLC affiliates all categories and is relatively prevalent. Thus, ALK inhibitors, such as Ceritinib and Alectinib, have been developed for treating NSCLC and distributed to the patients (Shaw et al. 2014; Kim et al. 2016).

Recently, Zeng et al. reported that ALK pathway is up-regulated in patients with sepsis, and inhibition of ALK-STING pathway protects against lethal endotoxemia and sepsis in mice (Zeng et al. 2017). Moreover, my prior study demonstrated that ALK impedes autophagosome maturation and increases tau accumulation, thus causing tau-mediated neurodegeneration and memory impairment in AD models. Paradoxically, though ALK is highly expressed in the brain and neurons and *Alk* knockout mice show enhanced brain function compared to control mice, its role was largely investigated and implicated in cancers.

In addition, despite massive researches on the function of ALK in disease, including oncogenesis, and other physiology, ALK has been known as an orphan receptor for years. Now, a few ALK ligands have been reported. Hesitation behavior 1 (HEN-1) bind s to SCD-2, *Caenorhabditis elegans* ortholog of ALK, and mediates synapse formation and sensory behavioral response (Liao et al. 2004; Ishihara et al. 2002). Jelly belly (Jeb) was reported to bind to ALK of *Drosophila melanogaster* and its downstream signaling is involved in embryonic visceral muscle and neuromuscular junction development (Lee et al. 2003; Rohrbough and Broadie 2010). Once, heparin-binding proteins pleiotropin and midkine were considered as ligands for vertebrate ALK. However, it turned out to be false (Kuo et al. 2007; Moog-

Lutz et al. 2005). Recent researches also revealed that heparin and FAM150A/B bind to and activate human ALK (Murray et al. 2015; Guan et al. 2015). Notably, secreted ALKAL, a zebrafish ortholog of FAM150A, was shown to function as a ligand to ALK *in vivo* in the neural crest of zebrafish (Fadeev et al. 2018). Although two ALK ligands have been uncovered, questions on these ligands still exists since *in vivo* function of heparin as a ligand for ALK has not been validated. Protein expression of ALKAL (FAM150A) in the nerve system, where most ALK proteins express, is also unclear in humans. In the absence of reliable ALK ligands, there are limitations in studying the *in vivo* functions of ALK activation or inhibition. Therefore, it is crucial to develop methods to activate or inhibit ALK.

To isolate ALK inhibitor or activator, I employed three ways. First, in collaboration with LegoChemBio Inc. I developed ALK inhibitor targeting its active site using ALK-inhibitor *in silico* modeling. Second, I screened small molecule library to isolate allosteric inhibitor of ALK targeting non-active site using reporter assay of ALK-ERK-Elk signaling axis. Third, in collaboration with K-bio, I generated agonistic and/or antagonistic ALK antibodies using a phage display antibody library panning. From the experiments, I found 2 novel non-active site ALK inhibitors from screening 1,568 compounds. Also, I found one compound KRCA0605 as an ALK

inhibitor targeting the hinge of ALK active site and attenuating memory impairment in 3xTg-AD mice. In addition, I found that 6 ALK antibodies generated from phage display library bound to human ALK on cells and two of them activate ALK and enhance tau accumulation. Together, those newly identified ALK inhibitors and antibodies are expected to be useful for exploiting the *in vivo* and pathologic function of ALK.

Results

II-1. Isolation of active site-targeting ALK inhibitors and their activity to ameliorate tau-mediated memory impairment

Isolation of active-site targeting ALK inhibitor using ALK-inhibitor docking model

Prevalent ALK inhibitors, such as Ceritinib and Alectinib, are ATP homologues and thus bind to ATP-binding site and inhibit kinase activity of ALK. In collaboration, LegoChemBio Inc. developed ALK protein modeling through ALK-inhibitor docking study. From the *in silico* model study, LegoChemBio Inc. newly synthesized KRCA0605 and found that KRCA0605 effectively bound to ALK hinge region (Figure II-1). KRCA0605 was verified to inhibit ALK enzyme activity *in vitro* and induced cell death in cancer cell lines. In addition, KRCA0605 has high B.B.B. permeability and plasma stability when injected intravenously and orally into rats and mice, respectively. These chemical properties make KRCA0605 suitable for cancer therapy as well as treating Alzheimer's disease.

Therefore, I decided to test the effect of KRCA0605 on ALK activity

and ALK-mediated tau accumulation. I conformed that KRCA0605 effectively inhibited autophosphoryaltion of ALK in SH-SY5Y neuronal cell line (Figure II-2). KRCA0605 was more effective to inhibit ALK activity than LDK378 at low concentration. More, I found that KRC0605 also interfered ALK-mediated tau phosphorylation (PHF-1) and accumulation (tau) in SH-SY5Y cells (Figure II-2). However, this inhibition on tau levels was not better than LDK378. These results indicate that KRC0605 inhibits ALK activation and tau accumulation in SH-SY5Y neuronal cells.

Oral administration of KRCA0605 alleviates tau accumulation and memory impairment of 3xTg-AD mice

Next, I tested *in vivo* effect of KRCA0605 on tau pathology and memory impairment in 3xTg-AD mice, an AD mice model that express APP, Presenilin and tau (Oddo et al. 2003). Since KRCA0605 fairly penetrates B.B.B. and good plasma stability, I orally administrated 7-month-old 3xTg-AD mice and age-matched wild-type mice every day with KRCA0605 (10 m.p.k.) for a month. The results of behavior tests revealed that KRCA0605 significantly alleviated space memory impairment in 3xTg-AD mice in the Y-maze test and recognition memory impairment in the novel object recognition test (Figure II-3A, B).

Moreover, western blot analysis of hippocampal tissue extracts prepared from the mice revealed that KRCA0605 decreased the amounts of total tau protein (HT7) and phosphorylated tau (PHF-1) in 3xTg-AD mice (Figure II-3C). Unlike these changes, there was not much change in the amount of pThr231-tau. These results indicate that KRCA0605 shows an inhibitory effect on memory impairment and concomitant tau accumulation in 3xAD mice.

II-2. Isolation of non-active site targeting ALK inhibitors

Isolation of ALK inhibitors using cell-based assay employing ALK-ERK-Elk1 axis

Since all ALK inhibitors, including KRCA0605, target active site of ALK protein, there has been an issue on the selectivity of the inhibitor in a similar kinase family. Given that AD is a chronic disease that needs treatment for a long time, I believed that allosteric inhibitors might be a better choice of therapeutics against AD and thus decided to isolate non-active site targeting ALK inhibitor. One of the most well-known downstream signals of ALK is the ERK pathway. When ALK is activated and auto-phosphorylated, SH2-

domain-containing proteins IRS1, SRC, and SHC bind to specific tyrosine residues of ALK (Lin, Riely, and Shaw 2017). Those ALK-bound SH2 proteins enhance phosphorylation of ERK1 and ERK2 through SRC or RAS (Johnson et al. 2014). Then, activated ERK sends down signaling via MSK, PI4K2, Elk, EIF43-BP and HDAC6. Using the ALK-ERK-Elk1 signaling, I established a cell-based screening assay to isolate ALK inhibitors. When SH-SY5Y cells are cotransfected with pFA2-Elk1-Gal4 (Elk1 fusion trans-activator), pRF-EGFP (Reporter), and ALK, ALK phosphorylates Elk1-GAL4dbd through ERK and the phosphorylated Elk1-GAL4dbd binds as a dimer to GAL4 UAS, leading to activation of transcription of the pRF-EGFP (Figure II-4A). Thus, ALK inhibitors could effectively reduce GFP fluorescence, a reporter activity, in the ALK-ERK-Elk1 axis. As expected, the expression of wild-type ALK or constitutive active BRAFV600E mutant enhanced the fluorescence, while the activity-dead ALK mutant failed to do so (Figure II-4B).

Using this cell-based reporter assay, I started to isolate ALK inhibitor by screening small molecule library. I chose B.B.B.-penetrating compound library that was purchased from ChemBridge Inc. Using this method, I screened 1,568 B.B.B.-penetrating compounds and found 25 small molecules that potentially inhibited the fluorescence in the cell-based assay (Figure II-

5A). After the secondary screening, I could isolate 5 small molecules that seemed to reduce the fluorescence by half (Figure II-5B). Subsequent analysis showed that #5 compound seemed to be toxic to SH-SY5Y cells at 50 μM for 48 h (Figure II-6).

The compounds inhibit ALK autophosphorylation and tau accumulation in neuronal cells

However, the decrease of reporter GFP fluorescence by compound does not always indicate that the compound inhibits ALK, because the compound might also interfere with the ALK-ERK-Elk1 signaling axis. Thus I assessed the effect of the compound on ALK activity in SH-SY5Y cells. While, the compounds #1, #2, and #5 reduced the activation of ALK in SH-SY5Y cells transiently expressing ALK (Figure II-7A), but did not affect the activation of constitutive active ALK.Fc mutant lacking the extracellular domain of ALK and, instead, harboring IgG Fc region (Figure II-7B). These results indicate that those compounds might target non-active site and extracellular region of ALK to inhibit it.

Given that ALK increases tau accumulation and phosphorylation, I assessed the effect of the compounds on tau accumulation. As expected,

western blot assays revealed that compound #1 reduced tau accumulation (Figure II-8A). More, using filter trap assay, I found that compound #1 decreased ALK-mediated tau aggregation in SH-SY5Y cells (Figure II-8B). In addition, from tau aggregation dot formation assay, I found that compounds #1 and #2 showed a great inhibitory effect on tau dot formation triggered by ALK in SH-SY5Y cells (Figure II-9). Since GFP-tau dot formation is prone to increase in stressed cells, a decrease of GFP-tau aggregation by compound #5 might be an indirect effect.

The compound affects ALK activity through the extracellular domain of ALK *in vitro*

The initial purpose of this screening was to find novel compounds that interfere with ALK activity through allosteric inhibition of ALK. Thus, I designed another assay to examine whether the compound could affect the kinase activity of ALK using truncated ALK protein harboring only the kinase domain but lacking the extracellular domain of ALK. Unlike LDK378, all the other compounds did not inhibit ALK activity even at higher concentrations than LDK378, showing less that than 10% of LDK 378 (Figure II-10). The results indicate that the newly discovered compounds might inhibit ALK and thus tau pathology through the extracellular domain of ALK.

II-3. Isolation and validation of ALK agonistic/antagonistic antibodies

Isolation of ALK antibodies with phage display

Despite some reports on the identification of ALK ligand, there is no good consensus on the ligand of ALK. Since ALK becomes a new pathogenic receptor for tau proteinopathy and can serve as a novel therapeutic target for the treatment of AD, I decided to develop ALK agonistic and antagonistic antibodies. In addition, current ALK inhibitors, including LDK378 and available other ALK inhibitors, were developed against active site of ALK and are thus ATP analogue, showing non-target effects by interfering with other kinases. In collaboration with Dr. DY Kim in K-BIO, several rounds of phage display antibody library panning were performed and putative clones interacting with immobilized human ALK protein were selected (Figure II-11).

I then examined for their abilities of those phage antibodies to bind to ALK expressed on the surface of SH-SY5Y cells (Figure II-12). FACS analysis revealed that like the positive antibody (mAb13) from biotech company, 7 (2A3, 2A10, 3B1, 3D2, and H11) out of 14 isolated phage

antibodies bound to full-length human ALK on SH-SY5Y cells (Figure II-12).

ALK antibodies affect ALK activity and tau aggregation

Next, I investigated whether those antibodies affect ALK activity in SH-SY5Y cells stably expressing human ALK. Western blot assay revealed that most of the antibodies seemed to enhance autophosphorylation of ALK in SH-SY5Y cells (Figure II-13A). Among them, treatment with 3D2 antibody showed the highest activity to induce ALK autophosphorylaiton (Figure II-13B). In addition, I also examined their effects on tau accumulation in the same cells. Interestingly, I found that treatment with 2A3 or 2A10 antibody increased the amounts of total tau protein (Tau) (Figure II-14A, B) and the phosphorylated tau (P-Tau S396) (Figure II-14A, C) in SH-SY5Y cells infected with GFP-tau lentivirus. Thus, it is likely that 2A3 and 2A10 antibodies bind to ALK on the cell surface to activate ALK and to increase tau accumulation.

Figure II-1. Schematic overview of KRCA0605 identification as an ALK inhibitor.

Discovery scheme and investigation of chemical properties of KRCA0605.

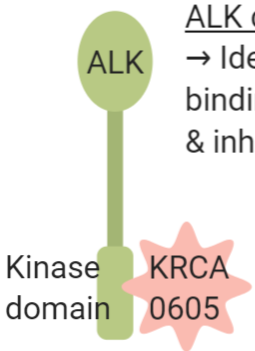

ALK docking study
→ Identification of KRCA0605 binding to hinge region & inhibiting kinase activity of ALK

Verified
1. ALK inhibition in vitro
2. ALK inhibition in cancer cell line
3. Plasma stability
4. Mouse BBB penetration

Figure II-2. Inhibitory effects of KRCA0605 on ALK-mediated tau phosphorylation in neuronal cells.

SH-SY5Y cells were cotransfected with GFP-tau (250 ng) and of ALK.Fc 750 ng) for 6 h and then treated with the indicated concentrations of either LDK378 (a positive control of Novartis) or KRCA0605 for additional 18 h. Following further incubation in fresh media for 6 h, cell lysates were prepared and subject to western blot analysis using anti-tau and ALK antibodies. GFP-tau was included in all transfections.

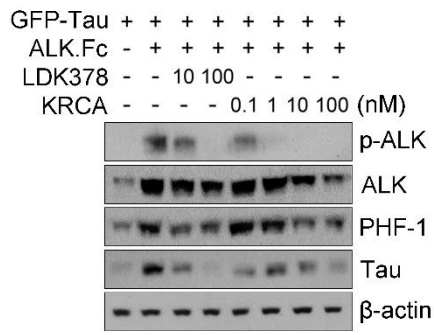
GFP-Tau + + + + + + + +
ALK.Fc - + + + + + + +
LDK378 - - 10 100 - - - -
KRCA - - - - 0.1 1 10 100 (nM)
p-ALK
ALK
PHF-1
Tau
β-actin

Figure II-3. Oral administration of KRCA0605 inhibits ALK-mediated memory impairment and tau pathology.

(A-C) The 7-month-old wild-type (WT) and 3xTg-AD mice were orally administrated every day with control PBS or KRCA0605 (10 mg/kg) for a month, and then examined for their behavior with Y-maze test (A) and novel object test (B) (WT/PBS, n = 9; WT/KRCA, n = 9; 3xTg-AD/PBS, n = 4; 3xTg-AD/KRCA, n = 10). Bars represent mean values ± S.D. One-tailed t-test. *P<0.05 (A). Two-way ANOVA. Bonferroni posttests. ***P<0.001 (B). After the behavioral tests, mice were sacrificed and hippocampal extracts were subjected to western blotting (C).

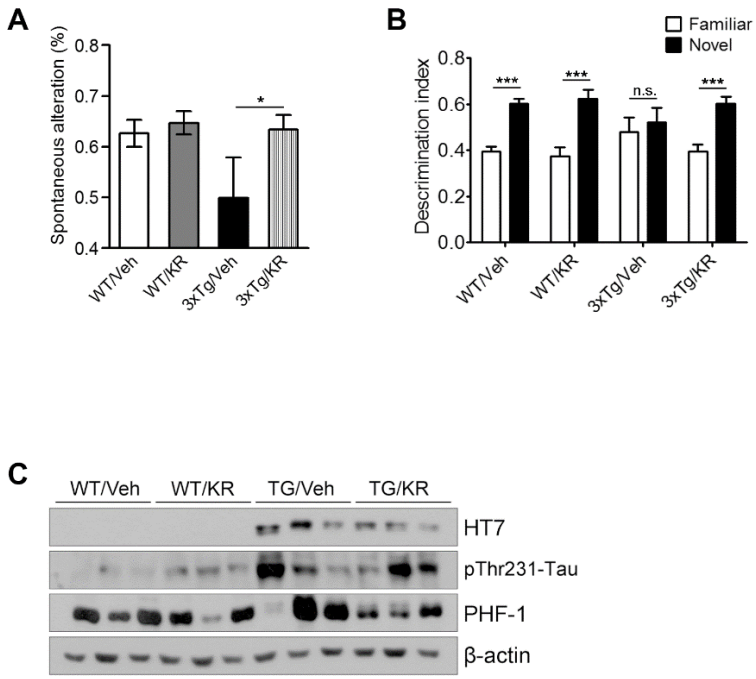
A
Spontaneous alteration (%)
0.8
0.7
0.6
0.5
0.4
*
WT/Veh
WT/KR
3xTg/Veh
3xTg/KR
B
Familiar
Novel
Descrimination index
0.8
0.6
0.4
0.2
0.0
***
***
n.s.
***
WT/Veh
WT/KR
3xTg/Veh
3xTg/KR

C
WT/Veh
WT/KR
TG/Veh
TG/KR
HT7
pThr231-Tau
PHF-1
β-actin

Figure II-4. Schematic diagram showing screening strategy of ALK inhibitors and control assay.

(A) Schematic overview depicting the procedure for ALK inhibitor screening strategy.

(B) HEK293T cells were cotransfected with FA2-Elk1-Gal4, RF-EGFP and either pcDNA3 (control), ALK, or its mutant for 24 h, and then observed for green fluorescence under fluorescent microscope. BRAF V600E was served as a positive control.

A

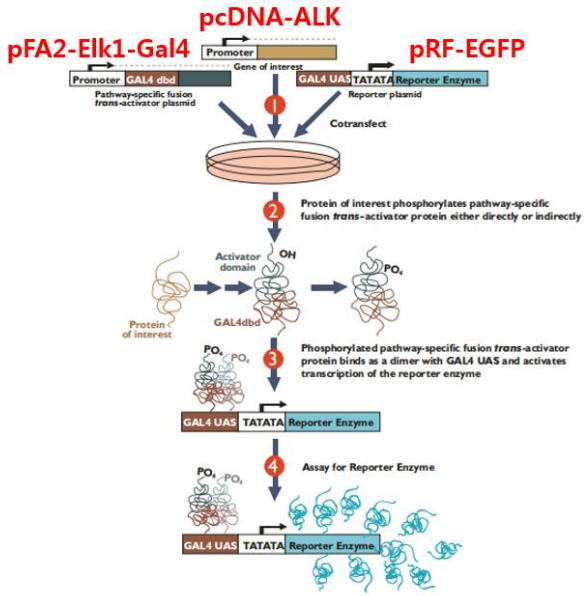
pcDNA-ALK
pFA2-Elk1-Gal4
Promoter
Gene of interest
Promoter GAL4 dbd
Pathway-specific fusion trans-activator plasmid
GAL4 UAS TATATA Reporter Enzyme
Reporter plasmid
pRF-EGFP
1
Cotransfect
2
Protein of interest phosphorylates pathway-specific fusion trans-activator protein either directly or indirectly
Activator domain
OH
PO4
Protein of interest
GAL4dbd
3
Phosphorylated pathway-specific fusion trans-activator protein binds as a dimer with GAL4 UAS and activates transcription of the reporter enzyme
GAL4 UAS TATATA Reporter Enzyme
4
Assay for Reporter Enzyme
GAL4 UAS TATATA Reporter Enzyme

B

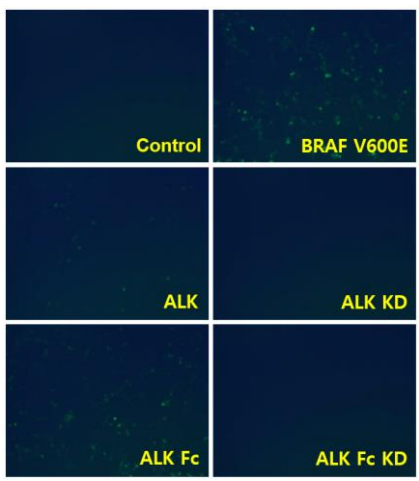
Control
BRAF V600E
ALK
ALK KD
ALK Fc
ALK Fc KD

Figure II-5. Primary and secondary screenings for ALK inhibitors with the FA2-Elk1-GAL4/RF-GFP assays.

(A) Primary screening results. HEK293T cells were cotransfected with pFA2-Elk1-Gal4, pRF-EGFP, and pcDNA-ALK and treated with DMSO (negative control), 500 nM Ceritinib (positive control), or 10 μM small molecules (Chembridge CNS set) for 24 h. Cells were then measured for green fluorescence with IN Cell Analyzer 2000. (B) Secondary screening results. The putative positive compounds were selected and were tested again using the FA2-Elk1-Gal4/RF-EGFP assay. Ceritinib was included as a positive control in all experiments.

A

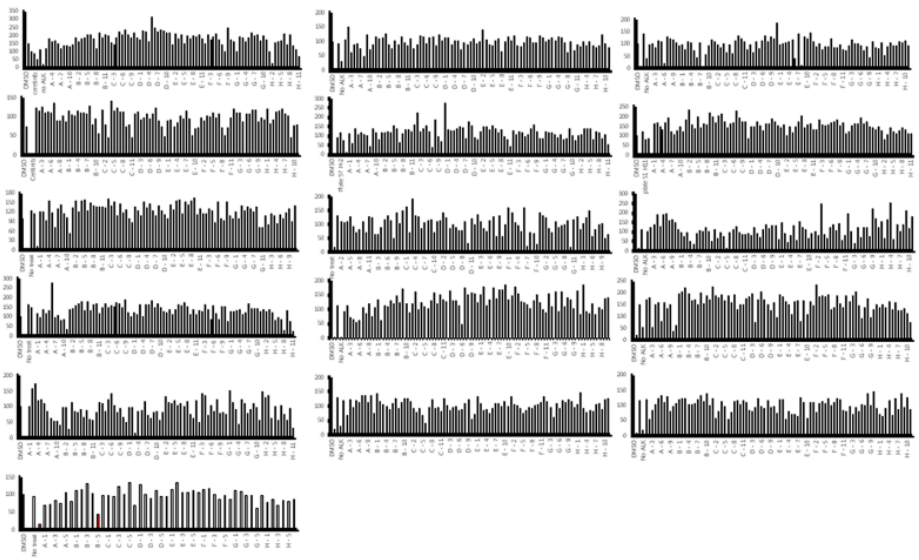

B

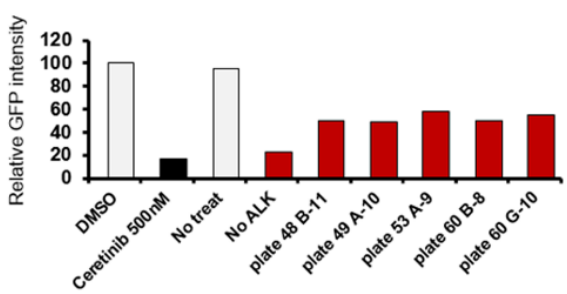
Relative GFP intensity
120
100
80
60
40
20
0
DMSO
Ceretinib 500nM
No treat
No ALK
plate 48 B-11
plate 49 A-10
plate 53 A-9
plate 60 B-8
plate 60 G-10

Figure II-6. Cell toxicity of the isolated compounds.

SH-SY5Y cells were treated with either DMSO, 10 nM LDK378, or 50 μM compounds for 48 h. Cell morphologies were observed under microscope. Bars depict 100 μm.

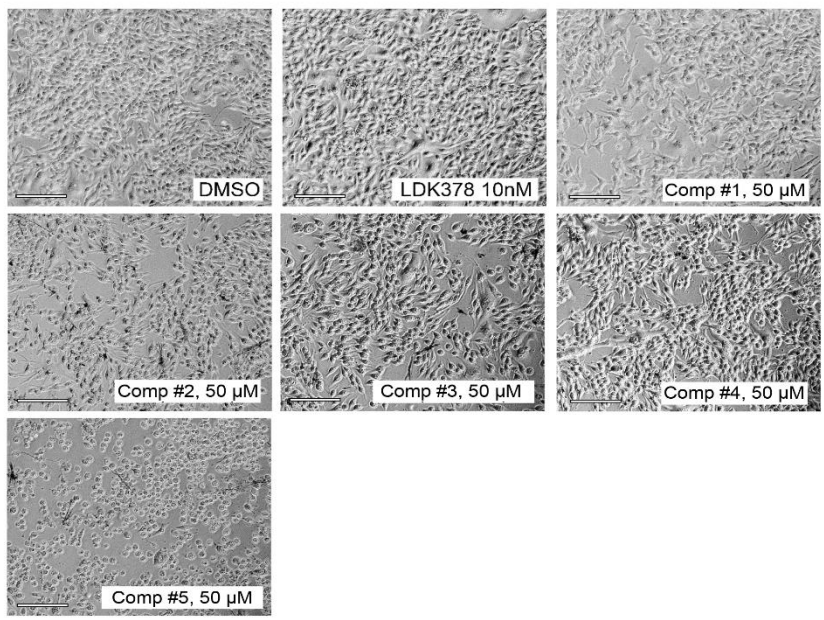
DMSO
LDK378 10nM
Comp #1, 50 µM
Comp #2, 50 µM
Comp #3, 50 µM
Comp #4, 50 µM
Comp #5, 50 µM

Figure II-7. Effects of the isolated compounds on the auto-phosphorylation of ALK and ALK.Fc.

(A) SH-SY5Y cells were transfected with control vector or ALK for 12 h and then left untreated or treated with the candidate compounds (10 μM) for 24 h. Cells were harvested and analyzed by western blotting.

(B) SH-SY5Y cells were transfected with control vector or ALK.Fc for 12 h and then left untreated or treated with the candidate compounds (10 μM) for 24 h. Cells were harvested and analyzed by western blotting.

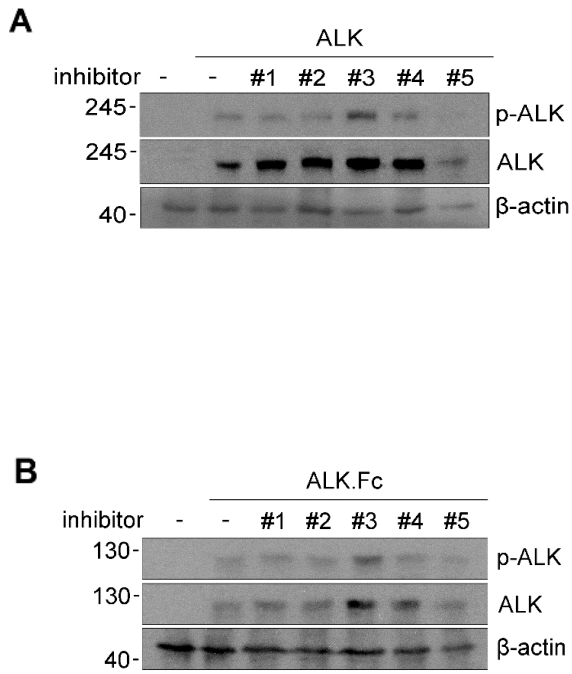
A
ALK
inhibitor - - #1 #2 #3 #4 #5
245-
245-
40-
p-ALK
ALK
β-actin
B
ALK.Fc
inhibitor - - #1 #2 #3 #4 #5
130-
130-
40-
p-ALK
ALK
β-actin

Figure II-8. Effects of the isolated candidates on tau accumulation and aggregation.

(A) SH-SY5Y cells were transfected with ALK for 12 h and then left untreated or treated with either LDK378 (10, 100 nM) or the candidate compounds (10 μM) for 24 h. Cells were harvested and analyzed by western blotting.

(B) SH-SY5Y cells were transfected with ALK and GFP-tau for 12 and left untreated or treated with the candidate compounds (10 μM) for 48 h. Cells were harvested and subject to filter trap assay.

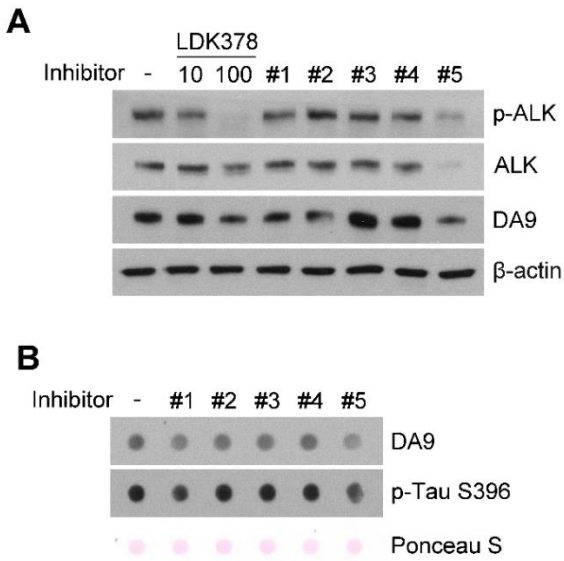
A
LDK378
Inhibitor - 10 100 #1 #2 #3 #4 #5
p-ALK
ALK
DA9
β-actin
B
Inhibitor - #1 #2 #3 #4 #5
DA9
p-Tau S396
Ponceau S

Figure II-9. Effects of the isolated compounds on ALK-mediated tau aggregation.

SH-SY5Y cells were cotransfected for 12 h with either empty vector or human ALK full length. Cells were treated with indicated compound (LDK378 : 10 nM, Compound #1-5 : 10 μM) for 30 h. GFP-positive dots are considered as tau aggregation and the number of the dots is counted.

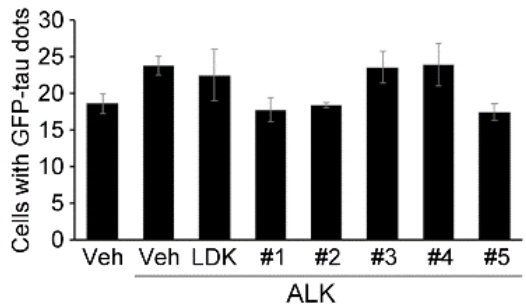
Cells with GFP-tau dots
30
25
20
15
10
5
0
Veh
Veh
LDK
#1
#2
#3
#4
#5
ALK

Figure II-10. In vitro ALK kinase activity assay using purified ALK kinase domain.

Purified ALK kinase domains (10 ug/ml) were incubated with the indicated concentrations of LDK378 (a positive control) and the compounds for 1 h, and measured for the inhibitory effect on catalytic activity of purified truncated human ALK. The inhibitory activity of LDK378 was set to 100% and others were relative to that of LDK378.

	Concentration (nM)	Inhibition (%)
comp#1	10000	19
	1000	19
comp#2	10000	7
	1000	9
comp#3	10000	10
	1000	-1
comp#4	10000	12
	1000	-10
comp#5	10000	6
	1000	8
LDK378	100	104
	10	98

Figure II-11. Graphical overview for antibody generation by a phage display antibody library panning.

Extracellular cellular domain of human ALK protein was produced, purified and subjected to phage display to isolate ALK antibody. Phages displaying antibody which are able to interact with extracellular domain of human ALK protein were selected from antibody phage display library. After several rounds of panning, the specific sequences of the phages were identified and subcloned into immunoglobulin expression vector to express the antibodies.

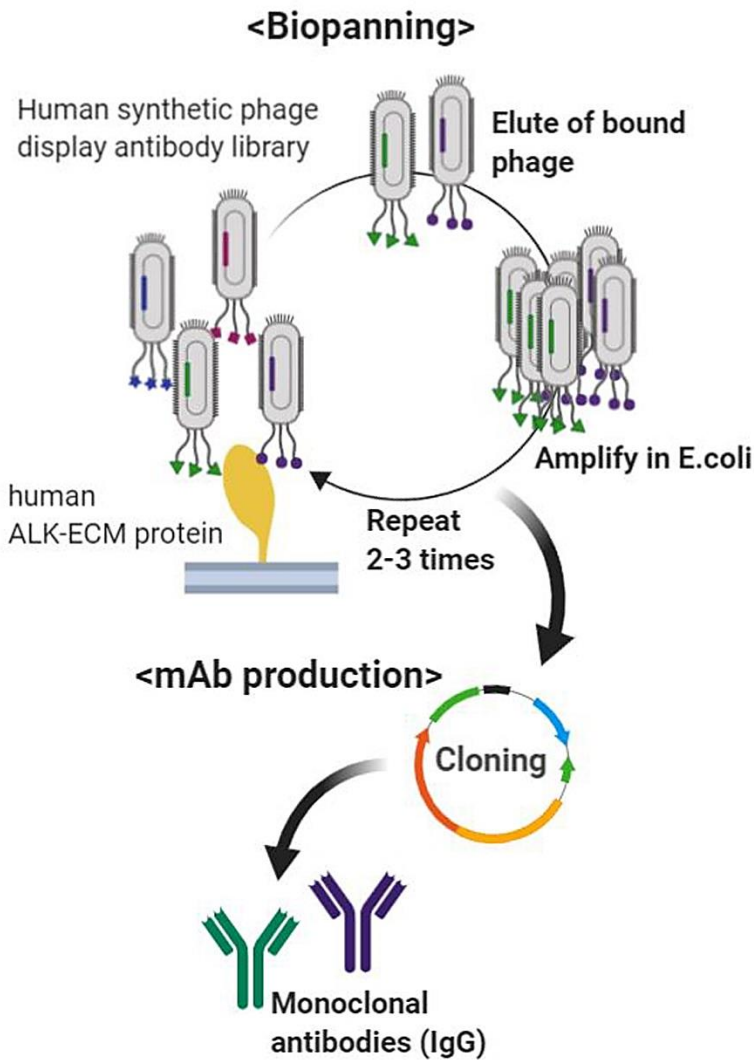
<Biopanning>
Human synthetic phage display antibody library
Elute of bound phage
Amplify in E.coli
human ALK-ECM protein
Repeat 2-3 times
<mAb production>
Cloning
Monoclonal antibodies (IgG)

Figure II-12. FACS analysis testing the binding of the antibodies to ALK on cell surface.

HEK293T cells were transfected with full-length human ALK for 24 h. After blocking cells (10^6 cell/ea) and phages ($2x10^{11}$/ea) for 30 min at 4 °C, cells were further incubated with the phage for 4 h at 4 °C and anti-M13-FITC (0.4 mg/mL) for 1 h at 4 °C. Cells were washed and analyzed for FITC fluorescence intensity with BD FACSAria™ III (BD Biosciences).

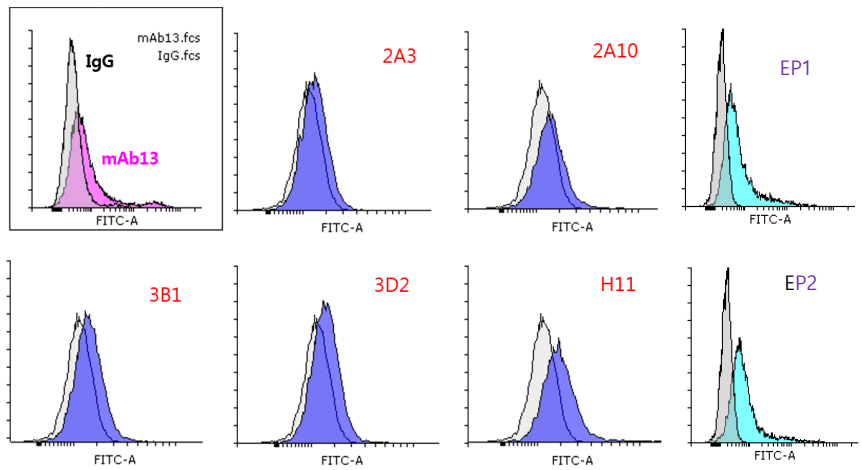
mAb13.fcs
IgG.fcs
IgG
mAb13
FITC-A
2A3
FITC-A
2A10
FITC-A
EP1
FITC-A
3B1
FITC-A
3D2
FITC-A
H11
FITC-A
EP2
FITC-A

Figure II-13. Antagonistic/agonistic effect of ALK antibodies.

(A) SH-SY5Y cells stably expressing full-length human ALK were incubated with 5 or 10 μM of IgG or the indicated antibodies for 20 min. Cell lysates were prepared and subject to western blot analysis.

(B) The signals of p-ALK and ALK on the blots were quantified by densitometric analysis. Bars represent relative ratios of p-ALK to ALK.

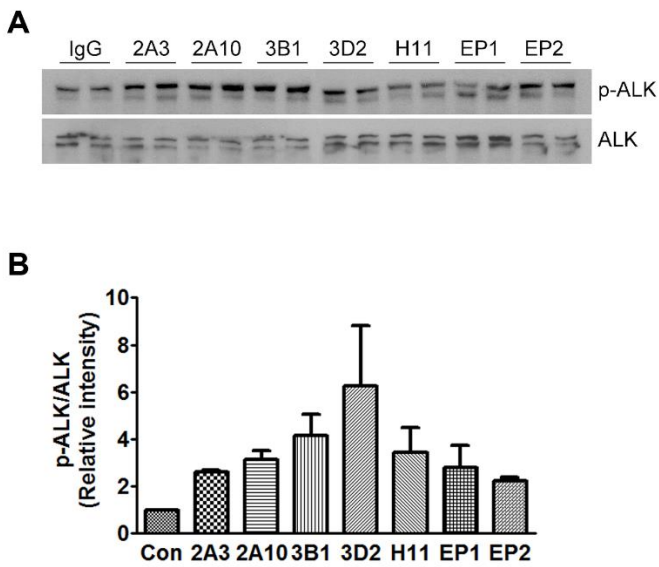
A
IgG
2A3
2A10
3B1
3D2
H11
EP1
EP2
p-ALK
ALK
B
p-ALK/ALK
(Relative intensity)
10
8
6
4
2
0
Con
2A3
2A10
3B1
3D2
H11
EP1
EP2

Figure II-14. Effects of the ALK antibodies on tau accumulation.

(A) SH-SY5Y cells stably expressing full-length human ALK were infected with GFP-tau adenovirus for 9 h and then treated with 5 or 10 μM of ALK antibodies for additional 24 h. Cell lysates were subject to western blot analysis.

(B, C) The signals of tau (B) or p-tau (S396) on the blots were measured by densitometric analysis and normalized by that of β-actin.

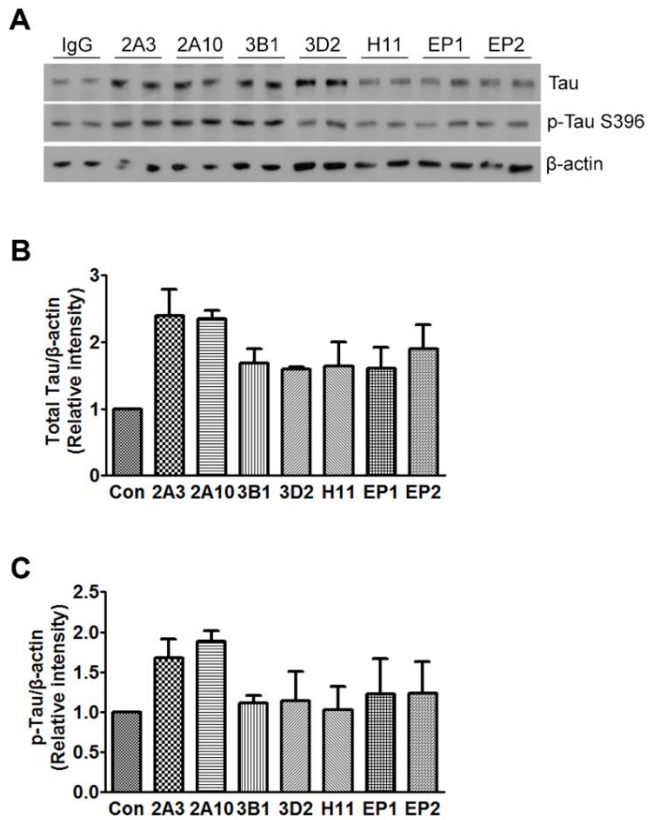
A
IgG
2A3
2A10
3B1
3D2
H11
EP1
EP2
Tau
p-Tau S396
β-actin
B
Total Tau/β-actin
(Relative Intensity)
0
1
2
3
Con 2A3 2A10 3B1 3D2 H11 EP1 EP2
C
p-Tau/β-actin
(Relative Intensity)
0.0
0.5
1.0
1.5
2.0
2.5
Con 2A3 2A10 3B1 3D2 H11 EP1 EP2

Figure II-15. Summary on small molecule inhibitors and antibodies of ALK.

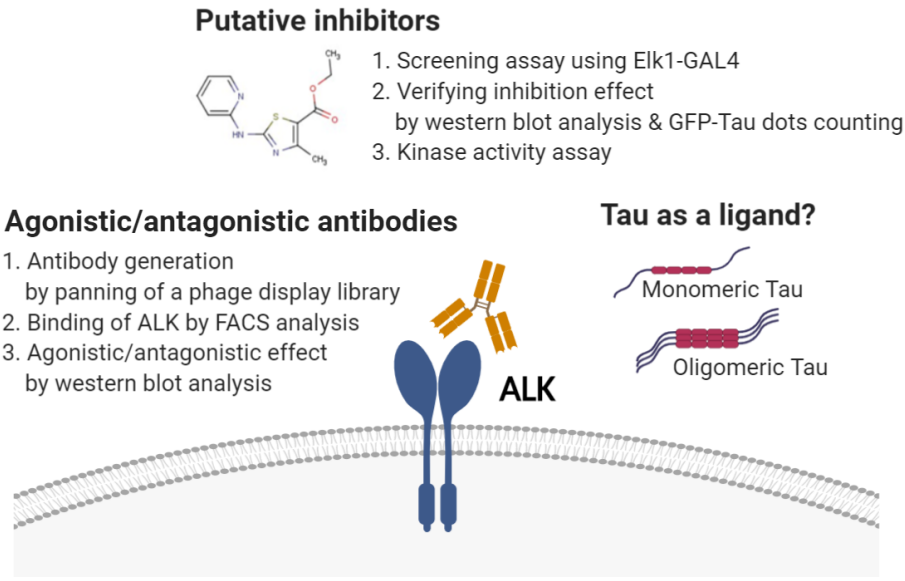
Putative inhibitors
1. Screening assay using Elk1-GAL4
2. Verifying inhibition effect
by western blot analysis & GFP-Tau dots counting
3. Kinase activity assay
Agonistic/antagonistic antibodies
1. Antibody generation
by panning of a phage display library
2. Binding of ALK by FACS analysis
3. Agonistic/antagonistic effect
by western blot analysis
ALK
Tau as a ligand?
Monomeric Tau
Oligomeric Tau

Discussion

As ALK plays a crucial role in neuron development and pathogenesis of various diseases, including tumorigenesis and AD, tools regulating ALK activity *in vitro* and *in vivo* are largely needed for functional study of ALK and therapeutic purposes. More importantly, the experimental tools are very useful for studying the molecular mechanism of ALK-mediated pathophysiologic signaling. As an example, I could elucidate *in vivo* role of ALK using pathophysiologic effect of KRCA0605, an active site inhibitor of ALK, in animal disease models. Especially, I could show that oral administration of KRCA0605 recovered memory defects and decrease tau accumulation in 3xTg-AD mice. These results demonstrate the *in vivo* role of ALK in tau pathology of AD model mice, confirming my previous results. At the same time, KRCA0605 could serve as a new therapeutic opportunity in the future.

Fortunately, it seemed that I discovered non-active site allosteric inhibitor of ALK via cell-based reporter assay. The compounds are expected to be specific to full-length ALK but do not regulate the catalytic activity of ALK *in vitro* and in the cell-based kinase assay. Actually, it needs more analysis measuring a direct binding of the compound to ALK protein and binding affinity. I have the structural formula for these compounds and need

more work to analyze whether there is a common motif in structure, and how the compound interacts and interferes with ALK. Nonetheless, if this compound functions as an allosteric inhibitor, it will be greatly exciting in that I may go through further for developing AD therapeutics. Though regulating kinase activity is highly effective, it is possible to modulate other kinases, too. In general, neurodegenerative disease is a chronic disease, taking tens of years to be pathogenic and diseased. Thus, a strategy to develop active site inhibitors against various kinases as AD therapeutics has a clear limitation.

In the same sense, the development of antagonistic ALK antibodies as a therapeutic purpose in AD is a good choice. One time, There were agonistic (mAb30) and antagonistic antibodies (mAb46) (Moog-Lutz et al. 2005). Those antibodies were utilized to characterize ALK signaling mainly in cancers. Unfortunately, the antibodies are not available anymore. Small molecule inhibitors against receptor tyrosine kinases (RTK) usually target the active site of the RTKs. On the other hand, there are fairly good antibodies for therapeutics against RTK and cell surface receptors in many cancers. I found that at least 4 antibodies were able to activate ALK in a cell-based assay. But it is needed to validate its effect *in vivo* study. For *in vivo* test, the ability of these antibodies to bind to mouse ALK will be examined and, if they do, *i.c.v.* injected into the brains of wild-type mice or tau AD model mice. Then, the activation of ALK will be investigated through behavioral test and western

blot analysis. For development of antagonistic ALK antibodies, I will characterize more antibodies in the clones isolated from the screening of phage display library.

In addition, my preliminary data indicated that tau itself might act as a ligand of ALK by directly binding to it. Heparin-binding proteins are believed to bind to ALK and heparin itself is also able to bind to ALK. Meanwhile, heparin binds to tau to promote its oligomerization and heparin sulfate proteoglycans (HSPGs) also can bind to tau and mediate internalization and propagation of the protein. These results allow me to presume that ALK might be able to bind to tau protein or form a complex with heparin.

In conclusion, I propose that ALK is a novel and crucial mediator of tau proteinopathy in AD and manipulation of ALK activity through inhibitor might provide insight into the molecular pathogenesis of AD and therapeutic opportunity against AD.

Materials and methods

Cell culture

HT22 and SH-SY5Y cells were cultured in Dulbecco's Modified Eagles Medium (GE healthcare, Cat# SH30243.01) with 10% (v/v) fetal bovine serum (Thermo Fisher Scientific, Cat# 26140-079). Stably tau-expressing HT22 cells were maintained in media supplemented with 200 μg/ml hygromycin B (Sigma Aldrich, Cat# 31282-04-9) and tau expression was induced by the treatment with 1 μg/ml doxycycline (Sigma Aldrich, Cat# 10592-13-9). Primary mouse hippocampal neurons were cultured at embryonic day 17. Briefly, resected mouse brain hippocampi and cortices were trypsinized with 0.05% Trypsin-EDTA (Thermo Fisher Scientific, Cat# 25300-062) for 20 min and neuronal cells were transferred to neurobasal medium (Thermo Fisher Scientific, Cat# 21103049) containing B27 serum supplement (Thermo Fisher Scientific, Cat# 17504044) and seeded on twelve-well tissue culture plates at a density of 2×10^6 cells per well.

Generation of tau stable cell line

SH-SY5Y cells were transfected with GFP-Tau or full-length human ALK and cultivated in media supplemented with 1 mg/ml G418 (Gold Biotechnology, Cat# G-418-5) for 2 weeks to generate a mixed cell

population. A single cell was grown to form a stable cell line.

Construction of plasmids

Tau (2N4R), the human longest form, in mammalian expression pCI vector was provided by Dr. Akihiko Takashima (RIKEN, Japan). Tau cDNA was subcloned into pcDNA3-HA (Invitrogen), pGFP (Clontech) and pBIG2i containing the tetracycline-regulated promoter for regulating the expression of an inserted gene and the selection marker for hygromycin B to generate HA or GFP fusion protein (pHA-tau, pGFP-tau, and pBIG2i-tau, respectively) (Krishnamurthy and Johnson 2004). Mouse ALK in mammalian expression pME18S-FL3 (pmALK) was obtained from Dr. Tadashi Yamamoto (University of Tokyo, Japan) (Iwahara et al., 1997). Full-length human ALK (ALK) and kinase-dead mutant (ALK KD; originally named ALKΔATP) in which the invariant lysine residue (K1150) located in the ATP-binding region was mutated to alanine were provided by Dr. Anton Wellstein (Georgetown University, DC) (Kuo et al. 2007) and subcloned into pcDNA3.1/Myc-His (pALK and pALK KD, respectively). ALK chimera (ALK.Fc) containing mouse IgG 2b Fc domain instead of the extracellular domain of the receptor in pcDNA3.1 and its kinase-defective form (ALK.Fc KD; originally named ALK*.Fc) in pcDNA3.1 (pALK.Fc and pALK.Fc KD, respectively) were gifts from was a gift from Dr. Mel Vigny (INSERM U440, Paris) (Souttou et

al. 2001). ALK.Fc and ALK.Fc KD were subcloned into lentiviral pCSII-EF-MCS-IRES2-Venus vector for the production of lentivirus (pLenti-ALK.Fc and pLenti-ALK.Fc KD, respectively).

Transfection

Expression plasmids were transfected using Lipofectamine 2000 (Invitrogen) or Lipofector-pMax (Aptabio) following the manufacturer's instructions.

Western blot analysis

Cells were lysed in ice-cold RIPA buffer [50 mM Tris-Cl (pH 8.0), 15 mM NaCl, 1% Triton X-100, 0.5% sodium deoxycholate, 0.1% SDS, 1 mM PMSF and 1 μg/ml each of aprotinin, leupeptin and pepstatin A]. For ALK protein detection, cell lysates were incubated at 37 °C for 15 min after lysis. Cell lysates were clarified by centrifugation at 13,000*g* for 10 min, diluted in 2× SDS loading buffer [100 mM Tris-Cl (pH 6.8), 4% SDS, 20% glycerol, 0.01% bromophenol blue, and 10% β-mercaptoethanol], resolved by SDS-PAGE and transferred onto PVDF membrane.

Antibodies

The following anti-tau antibodies were used: DA9 (total Tau; generously provided by Dr. Peter Davies, Albert Einstein College of Medicine, NY),

phospho-Tau Ser396 (Invitrogen, Cat# 44-752G), LC3 (Novus Biologicals, Cat# NB600-1384), anti-SQSTM1 (Abnova, Cat# H00008878-M01), p-ALK (p-Tyr1604; Cell signaling, Cat# 3341), ALK1 (BD Pharmingen, Cat# 559254), ALK (Invitrogen, Cat# 51-3900), ALK (DAKO, IS64130-2), β-actin (Sigma Aldrich, Cat# A2668) and GFP (Santa Cruz, Cat# sc-8334).

Mice

WT (C57BL/6) and 3xTg-AD mice were used. Mice were raised under a 12 : 12 h light-dark cycle with free access to food and water *ad libitum*. All experiments involving animals were performed according to the protocols approved by the Seoul National University Institutional Animal Care and Use Committee (SNU IACUC) guidelines.

Lentivirus production

Lentiviral vector stock was produced in HEK 293FT cells following calcium phosphate-mediated transfection of the modified transfer vector, packing vectors pMDLg/pRRE and pCMV-VSV-G-RSV-Rev. Supernatants were harvested over 48 to 60 h and concentrated by ultracentrifugation at 50,000 *g* for 2 h at 4 °C. Virus titers were assessed by transducing HEK 293 cells with serial dilutions of viral stock.

In vitro assay of ALK activity

Mix 100 nl of 100X Test Compound (LDK378 and 5 prospecting ALK inhibitors) in 100% DMSO, 4 µl of Kinase buffer [50 mM HEPES pH 7.5, 0.01% BRIJ-35, 10 mM $MgCl_2$, 1 mM EGTA], 5 µL of 2X Peptide/Kinase Mixture and 2.5 µl of 4X ATP Solution [50 mM HEPES pH 7.5, 0.01% BRIJ-35, 10 mM MgCl2, 1 mM EGTA] in plate. The final 10 µL Kinase Reaction consists of 4.25 - 96 ng ALK. Shake the plate for 30 seconds and then incubate the plate for 60 min during kinase reaction. Add 5 µl of 1:256 dilution of Development Reagent Solution B and shake the plate for 30 seconds and incubate the plate for 60 min at room temperature. Finally, read on fluorescence plate reader and analyze the data.

Behavior tests

Y Maze Spontaneous Alternation Test. The mice were placed at the end of one arm and allowed to explore freely through the maze (32.5 cm length x 15 cm height) for 7 min. An entry occurs when all 4 paws are placed into the arm. The number of arm entries and the number of total alterations were recorded and calculated for the percentage. After each trial, the apparatus was cleaned with 70% ethanol.

2-Novel object recognition. During the habituation, the mice were allowed to move within an empty white plastic chamber (22 cm wide × 27 cm long × 30 cm high) for 7 min at 24-hour intervals. After 2 days, the mice were exposed to 2 objects and allowed to explore freely for 7 min. In the testing trial performed 24 h later, 1 of the familiar objects was replaced with a novel object and the time spent exploring each object was recorded during a 7-minute period. Between each trial, the arena and objects were wiped down with 70% ethanol.

Quantification and statistical analysis

Statistical analyses were conducted by using Prism. Data are expressed as mean ± S.E.M. Statistical comparisons between two groups were performed using two-tailed t-test and comparisons between multiple groups were performed using one-way analysis of variance (ANOVA) followed by Tukey's test as appropriate.

References

Chen, Y., J. Takita, Y. L. Choi, M. Kato, M. Ohira, M. Sanada, L. Wang, M. Soda, A. Kikuchi, T. Igarashi, A. Nakagawara, Y. Hayashi, H. Mano, and S. Ogawa. 2008. 'Oncogenic mutations of ALK kinase in neuroblastoma', *Nature*, 455: 971-4.

Fadeev, Andrey, Patricia Mendoza-Garcia, Uwe Irion, Jikui Guan, Kathrin Pfeifer, Stephanie Wiessner, Fabrizio Serluca, Ajeet Pratap Singh, Christiane Nüsslein-Volhard, and Ruth H. Palmer. 2018. 'ALKALs are in vivo ligands for ALK family receptor tyrosine kinases in the neural crest and derived cells', *Proceedings of the National Academy of Sciences*, 115: E630-E38.

George, R. E., T. Sanda, M. Hanna, S. Frohling, W. Luther, 2nd, J. Zhang, Y. Ahn, W. Zhou, W. B. London, P. McGrady, L. Xue, S. Zozulya, V. E. Gregor, T. R. Webb, N. S. Gray, D. G. Gilliland, L. Diller, H. Greulich, S. W. Morris, M. Meyerson, and A. T. Look. 2008. 'Activating mutations in ALK provide a therapeutic target in neuroblastoma', *Nature*, 455: 975-8.

Guan, J., G. Umapathy, Y. Yamazaki, G. Wolfstetter, P. Mendoza, K. Pfeifer, A. Mohammed, F. Hugosson, H. Zhang, A. W. Hsu, R. Halenbeck, B. Hallberg, and R. H. Palmer. 2015. 'FAM150A and FAM150B are

activating ligands for anaplastic lymphoma kinase', *Elife*, 4: e09811.

Hallberg, Bengt, and Ruth H. Palmer. 2013. 'Mechanistic insight into ALK receptor tyrosine kinase in human cancer biology', *Nature Reviews Cancer*, 13: 685.

Ishihara, T., Y. Iino, A. Mohri, I. Mori, K. Gengyo-Ando, S. Mitani, and I. Katsura. 2002. 'HEN-1, a secretory protein with an LDL receptor motif, regulates sensory integration and learning in Caenorhabditis elegans', *Cell*, 109: 639-49.

Iwahara, T., J. Fujimoto, D. Wen, R. Cupples, N. Bucay, T. Arakawa, S. Mori, B. Ratzkin, and T. Yamamoto. 1997. 'Molecular characterization of ALK, a receptor tyrosine kinase expressed specifically in the nervous system', *Oncogene*, 14: 439-49.

Johnson, G. L., T. J. Stuhlmiller, S. P. Angus, J. S. Zawistowski, and L. M. Graves. 2014. 'Molecular pathways: adaptive kinome reprogramming in response to targeted inhibition of the BRAF-MEK-ERK pathway in cancer', *Clin Cancer Res*, 20: 2516-22.

Kim, D. W., R. Mehra, D. S. W. Tan, E. Felip, L. Q. M. Chow, D. R. Camidge, J. Vansteenkiste, S. Sharma, T. De Pas, G. J. Riely, B. J. Solomon, J. Wolf, M. Thomas, M. Schuler, G. Liu, A. Santoro, S. Sutradhar, S. Li, T. Szczudlo, A. Yovine, and A. T. Shaw. 2016. 'Activity and safety of ceritinib in patients with ALK-rearranged non-small-cell lung cancer

(ASCEND-1): updated results from the multicentre, open-label, phase 1 trial', *Lancet Oncol*, 17: 452-63.

Krishnamurthy, P. K., and G. V. Johnson. 2004. 'Mutant (R406W) human tau is hyperphosphorylated and does not efficiently bind microtubules in a neuronal cortical cell model', *J Biol Chem*, 279: 7893-900.

Kuo, A. H., G. E. Stoica, A. T. Riegel, and A. Wellstein. 2007. 'Recruitment of insulin receptor substrate-1 and activation of NF-kappaB essential for midkine growth signaling through anaplastic lymphoma kinase', *Oncogene*, 26: 859-69.

Lee, H. H., A. Norris, J. B. Weiss, and M. Frasch. 2003. 'Jelly belly protein activates the receptor tyrosine kinase Alk to specify visceral muscle pioneers', *Nature*, 425: 507-12.

Liao, E. H., W. Hung, B. Abrams, and M. Zhen. 2004. 'An SCF-like ubiquitin ligase complex that controls presynaptic differentiation', *Nature*, 430: 345-50.

Lin, Jessica J., Gregory J. Riely, and Alice T. Shaw. 2017. 'Targeting ALK: Precision Medicine Takes on Drug Resistance', *Cancer Discovery*, 7: 137-55.

Moog-Lutz, C., J. Degoutin, J. Y. Gouzi, Y. Frobert, N. Brunet-de Carvalho, J. Bureau, C. Creminon, and M. Vigny. 2005. 'Activation and inhibition of anaplastic lymphoma kinase receptor tyrosine kinase by

monoclonal antibodies and absence of agonist activity of pleiotrophin', *J Biol Chem*, 280: 26039-48.

Morris, S. W., M. N. Kirstein, M. B. Valentine, K. G. Dittmer, D. N. Shapiro, D. L. Saltman, and A. T. Look. 1994. 'Fusion of a kinase gene, ALK, to a nucleolar protein gene, NPM, in non-Hodgkin's lymphoma', *Science*, 263: 1281-4.

Morris, S. W., C. Naeve, P. Mathew, P. L. James, M. N. Kirstein, X. Cui, and D. P. Witte. 1997. 'ALK, the chromosome 2 gene locus altered by the t(2;5) in non-Hodgkin's lymphoma, encodes a novel neural receptor tyrosine kinase that is highly related to leukocyte tyrosine kinase (LTK)', *Oncogene*, 14: 2175-88.

Motegi, A., J. Fujimoto, M. Kotani, H. Sakuraba, and T. Yamamoto. 2004. 'ALK receptor tyrosine kinase promotes cell growth and neurite outgrowth', *J Cell Sci*, 117: 3319-29.

Murray, P. B., I. Lax, A. Reshetnyak, G. F. Ligon, J. S. Lillquist, E. J. Natoli, Jr., X. Shi, E. Folta-Stogniew, M. Gunel, D. Alvarado, and J. Schlessinger. 2015. 'Heparin is an activating ligand of the orphan receptor tyrosine kinase ALK', *Sci Signal*, 8: ra6.

Oddo, S., A. Caccamo, J. D. Shepherd, M. P. Murphy, T. E. Golde, R. Kayed, R. Metherate, M. P. Mattson, Y. Akbari, and F. M. LaFerla. 2003. 'Triple-transgenic model of Alzheimer's disease with plaques and

tangles: intracellular Abeta and synaptic dysfunction', *Neuron*, 39: 409-21.

Rohrbough, Jeffrey, and Kendal Broadie. 2010. 'Anterograde Jelly belly ligand to Alk receptor signaling at developing synapses is regulated by Mind the gap', *Development*, 137: 3523-33.

Shaw, Alice T., Dong-Wan Kim, Ranee Mehra, Daniel S.W. Tan, Enriqueta Felip, Laura Q.M. Chow, D. Ross Camidge, Johan Vansteenkiste, Sunil Sharma, Tommaso De Pas, Gregory J. Riely, Benjamin J. Solomon, Juergen Wolf, Michael Thomas, Martin Schuler, Geoffrey Liu, Armando Santoro, Yvonne Y. Lau, Meredith Goldwasser, Anthony L. Boral, and Jeffrey A. Engelman. 2014. 'Ceritinib in ALK-Rearranged Non–Small-Cell Lung Cancer', *New England Journal of Medicine*, 370: 1189-97.

Souttou, B., N. B. Carvalho, D. Raulais, and M. Vigny. 2001. 'Activation of anaplastic lymphoma kinase receptor tyrosine kinase induces neuronal differentiation through the mitogen-activated protein kinase pathway', *J Biol Chem*, 276: 9526-31.

Zeng, L., R. Kang, S. Zhu, X. Wang, L. Cao, H. Wang, T. R. Billiar, J. Jiang, and D. Tang. 2017. 'ALK is a therapeutic target for lethal sepsis', *Sci Transl Med*, 9.

국문초록

타우 단백질은 Aβ (beta amyloid) 단백질과 더불어 알츠하이머병에서 보이는 가장 대표적인 병리적 단백질이다. 알츠하이머병을 겪고 있는 사람의 뇌에는 타우 단백질이 인산화되어 있거나, 더 나아가 타우 단백질끼리 뭉쳐서 생성된 응집체 (aggregates)가 발견된다. 인산화된 타우는 정상적인 타우보다 더 응집하기 쉬워서 매듭 형태를 이루기가 쉽기 때문에 높은 독성을 가진다고 여겨진다. 타우(tau)는 미소관 (microtubule)과 결합하여 안정화시키는 역할을 하는 단백질로, 타우 단백질의 인산화와 축적은 알츠하이머병에서 나타나는 기억력 손상 외에도 다양한 종류의 타우 병증 (tauopathy)와 신경퇴행성 질환과 연관되어 있다고 알려져 있다. 타우를 조절하는 기작에 대한 연구는 대부분 타우의 인산화를 조절하는 인산화 효소와 그 인산화 효소를 포함하는 신호 전달에 관한 것이다.

ALK (Anaplastic Lymphoma Kinase)는 후기 배아 단계에서 중추 신경계와 말초 신경계의 신경세포에서 발현되는 수용체인산화효소 (receptor kinase)이다. ALK가 돌연변이가 생기거나 다양한 단백질과 융합이 일어났을 때, 비소세포성 폐암, 신경아세포종 등과 같은 암을 일으키는 암유발인자로써 역할을 한다. 이처럼, 이전의 ALK 관련 연구는 ALK의 돌연변이 또는 융합 단백질 발현으로 인한 종양 형성에서의 역할에 대한 내용으로 국한되어 있다. 본 연구는 신경세포에서 발현되는 ALK가 타우 단백질의 과인산화와 축적을 조절하여 타우 단백질에 의한 신경세포의 병리학적 현상에서의 기능을

규명하였다.

본 실험실이 보유하고 있는 630개의 인산화 효소와 2,000개의 막단백질을 포함한 4,000개의 cDNA library를 대상으로 GFP-tau 응집 screening을 진행한 결과, 타우 응집을 증가시키는 유전자로 ALK를 발굴해 내었다. 더불어, 각각 6, 9, 12 개월 령의 야생형 쥐와 한배 새끼인 ALK 손실 쥐의 해마와 피질 조직을분석한 결과, ALK의 부재가 타우 단백질의 양을 감소시키는 것을 관찰하였다. 흥미롭게도, ALK에 의한 타우 단백질의 축적은 자가포식 소체의 저해로 인한 것임을 p62와 LC3-Ⅰ, LC3-Ⅱ 양이 증가하는 것을 통해 밝혔고, 또한 mCherry-GFP-LC3와 GFP-Stx17, RFP-LC3의 공존의 정도를 조사한 결과, ALK가 자가포식 소체가 자가용해 소체로 발달하는 것을 저해하는 것을 증명하였다. ALK의 downstream에 존재하여 신호 전달을 매개하는 단백질로 Grb2를 screening을 통해 발굴하였으며, Grb2와 ALK의 상호작용 또한 관찰하였다. ALK.Fc 과발현 시에 신경세포의 축색돌기에 LC3 양성인 부기가 발생하였고, 신경세포의 퇴화 (degeneration)의 표지가 되는 가지돌기 가시 밀도 (dendritic spine density)가 감소하는 것을 관찰하였다. 또한, 쥐 일차 신경세포에서 ALK agonistic antibody를 통해 ALK를 활성화시키면 세포 사멸이 증가하였다.

in vivo 에서 앞서 관찰한 내용을 재현하기 위해 5-6 개월령 야생형 쥐와 알츠하이머병모델인 3xTg-AD 에 stereotaxic 방식으로 ALK.Fc를 과발현하는 lentivirus를 주입하고 1 개월 후에 기억력과 타우 단백질의 변화를 관찰한 결과, 공간 기억력을 측정하는 Y-maze,

학습과 기억력을 측정하는 신물질 탐색 시험 (novel object recognition test), 명시적 기억능력검사인 수동 회피 실험 (passive avoidance test) 총 3가지 기억력 실험을 통해서 야생형과 3xTg-AD 모두에서 ALK 과발현 시킬 경우 기억력이 저해되었다. 기억력 실험 후, 쥐 뇌의 해마 부분 (Hippocampus)를 단백질 발현 분석법으로 분석 결과, 인산화된 타우의 양이 증가한 것 또한 확인하였다. 다음으로는 ALK의 억제가 생체 내에서 보이는 효과를 살펴보기 위해 7개월령 대조군인 야생형 쥐와 실험군인 3xTg-AD 쥐에 ALK의 저해제인 Ceritinib를 한 달간 복부 투여를 수행한 후, 쥐들의 기억력을 행동 실험을 통해서 조사한 결과, 알츠하이머 표현형을 가지는 3xTg-AD에서 떨어졌던 기억력이 Ceritinib을 투여했을 경우 대조군인 야생형 쥐의 기억력 정도로 회복하는 것을 확인하였다. 더불어 3xTg-AD에서 증가하였던 타우 단백질의 양과 인산화가 Ceritinib을 투여한 그룹에서는 현저히 줄어드는 것을 확인하였다.

나이 든 정상인과 알츠하이머병 환자의 해마 부분 뇌 조직을 단백질 발현 분석법을 통해서 분석한 결과, 정상인에 비해서 알츠하이머병 환자의 뇌 조직에서 훨씬 더 높은 ALK의 발현을 확인하였다 또한, 알츠하이머병 환자의 해마 조직을 면역조직화학 방법으로 조사한 결과, ALK와 신경섬유 매듭이 공존하고 있음을 발견하였다. 이러한 결과를 통해 ALK가 자가포식 소체의 성숙을 저해함으로써 타우 축적을 촉진하며, 신경세포에서의 세포사멸을 일으키고 알츠하이머병에서 보이는 타우 병리와도 연관성이 있음을 결론지을 수 있다.

앞의 결과를 통해서 ALK가 치매에서 보이는 타우에 의한 신경독성을 일으키는 원인이 된다는 것을 알 수 있었고, 치매 치료제의 첫 단계가 될 수 있는 새로운 ALK 저해제와 항체를 발굴, 조사하는 실험을 진행하였다. LegoChem Biosciences이 docking study를 통해 ALK의 hinge 부분에 결합하여 ALK의 키나아제 활성을 억제한다고 찾은 KRCA0605의 *in vivo*에서의 기능을 밝히는 실험을 수행하였다. 7개월령의 3xTg-AD 모델 쥐에 10 m.p.k.의 KRCA0605를 한 달간 경구투여 하였을 때, 3xTg-AD 모델 쥐의 손상된 기억력이 회복되는 것을 확인하였고, 또한 인산화된 타우와 전체 타우의 양이 줄어든 것을 확인할 수 있었다. 이 결과는 ALK의 타우를 통한 신경퇴행 기능을 다시 한번 확인시켜주며, KRCA0605의 치매 치료제로써의 가능성을 제시하였다.

또한, ALK가 과발현이 되었을 때 ERK를 통해 ELK1을 활성화하는 사실을 이용하여 새로운 ALK 저해 reporter assay를 고안하고 assay를 이용하여 BBB를 통과하는 1568개를 대상으로 screening을 진행하였고 이 중에 형광 세기를 낮추는 화합물로 총 5개를 발굴하였다. 단백질 발현 분석법을 통해서 5개의 화합물 모두 ALK를 저해하는 효과를 보이고, GFP-Tau를 이용한 tau dot counting 실험을 통해서는 1, 2, 5번의 화합물이 타우 응집을 억제하는 결과를 관찰하였다. 반면 *in vitro* kinase assay 결과에서는 해당 화합물들이 ALK의 인산화 효소 능력에는 아무런 영향도 끼치지 않는 것을 보아, ALK의 활성 자리가 아닌 부위를 대상으로 한다는 것을 유추할 수 있다.

ALK 저해제 발굴과 동시에 K-BIO 김대영 박사님

신항체발굴팀과 협업하여 ALK와 결합하는 항체 중에서 agonistic 혹은 antagonistic 효과를 보일 수 있는 항체를 발굴하는 실험을 진행한 결과 항체 library에서 human ALK와 결합할 수 있는 추정 상의 항체 14종을 선별하였고, FACS 분석법을 통해서 14종 중에 7종의 항체가 세포에서 발현된 ALK와 결합한다는 것을 확인하였다. 더 나아가 4종의 항체가 ALK를 활성화시키고 타우의 축적도 증가시키는 agonistic 항체임을 단백질 분석법을 통해 밝혔다.

위의 실험 결과들을 모두 종합하면, 알츠하이머병 발병에서 ALK가 가지는 역할과 기능을 새롭게 밝힘으로써 알츠하이머병이 발병하는 기작에 대한 이해를 높이고, 궁극적으로는 알츠하이머병에서 보이는 기억력 저하를 회복시킬 수 있는 치료제 개발에 대한 기반을 마련하였다.

주요어 : ALK, 타우 병증, 자가포식작용, 알츠하이머병,

학번 : 2012-23066